Geomorphology xxx (2013) xxx–xxx

Contents lists available at SciVerse ScienceDirect

Geomorphology

journal homepage: www.elsevier.com/locate/geomorph

Effects of active folding and reverse faulting on stream channel evolution, Santa Barbara Fold Belt, California

Benjamin L. Melosh [a,b,*], Edward A. Keller [a]

[a] Department of Earth Science, University of California, Santa Barbara, CA, 93101, United States
[b] Department of Earth and Planetary Science, McGill University, Montréal, Québec, H3A 2A7, Canada

ARTICLE INFO

Article history:
Received 24 March 2012
Received in revised form 21 December 2012
Accepted 26 December 2012
Available online xxxx

Keywords:
Stream incision
Uplift
Paleochannel
Santa Barbara Fold Belt (SBFB)
Fold propagation
Geomorphic indices

ABSTRACT

The Santa Barbara Fold Belt (SBFB) is an area of active crustal shortening comprising younger east–west and older southeast-northwest oriented reverse faults and folds. Changes in channel position and stream incision are the result of active fold growth and uplift. Rates of incision range from 0.4 ± 0.1 m/ka to 1.2 ± 0.04 m/ka. Lateral stream diversion from fold and fault growth varies from 6.7 to 0.4 km. Minimum uplift of western Mission Ridge anticline is 0.8 ± 0.1 m/ka and minimum uplift on the Mesa fault is 0.3–0.4 m/ka. The hypothesis that east-to-west folds are younger is suggested by a cross-cutting relationship and is tested using geomorphic indices of active tectonics including: valley width to height ratios (Vf), mountain front sinuosity (Smf) and drainage densities (Dd). East-to-west trending structures have mean values of Vf, Smf, and Dd of 2.7, 1.2, and 2.2 km/km^2, respectively, while southeast-to-northwest trending structures have mean values of 5.0, 1.5, and 3.7 km/km^2, respectively. We present a new geomorphic tool, the stream diversion index, which uses diversion timing and distance to assess relative tectonic activity; these values range from 6 to 260 m/ka. All of these values support the hypothesis that the east-to-west folds are younger and more active. Clockwise rotation of the Western Transverse Ranges is probably the process that produced the two sets of structures. With rotation the older set that started out east-to-west eventually became northwest-to-southeast, and more difficult to maintain with the north-to-south contractional (shortening) associated with the Big Bend of the San Andreas fault 80 km to the north. The second set of younger structures formed with a more favorable (east-to-west) orientation to the shortening.

1. Introduction

1.1. Research objectives, purpose and importance

Strain is accommodated in active fold and thrust belts primarily by offset along faults and secondarily by folding in the hanging wall. The geometry of the fault controls the shape and style of the overlying fold, which in turn controls the shape of the landscape (Keller and Pinter, 2002; Burbank and Anderson, 2012). Our ability to infer the presence and geometry of blind faults from the landscape is important because of the large seismic hazard they present (e.g. Keller and Gurrola, 2000; Keller and Pinter, 2002; DeVecchio and Keller, 2008; DeVecchio et al., 2012). We can also use hanging wall fold geometry and geomorphology to decipher the most-recent history of deformation in complex fold and thrust belts.

Because hanging wall folds represent a significant portion of strain it is important to understand their evolution when analyzing the development of an orogenic system as a whole. However, many active fold and thrust belts occur in urban settings, e.g. Los Angeles, or are covered by vegetation, e.g. foreland fold and thrust belts in the northern Andes. In such cases one tool we have at our disposal is a remote sensing based detailed geomorphic analysis of folds. One of the most important tools within this geomorphic toolbox is the analysis of stream patterns (e.g. Jackson et al., 1996; Keller et al., 1998, 1999; Keller and Pinter, 2002; Ramsey et al., 2008).

Analysis of river or stream incision and diversion provides valuable information about the development and evolution of folds and their underlying faults (e.g. Jackson et al., 1996; Boudiaf et al., 1998; Keller et al., 1998, 1999; Walker, 2006; Ramsey et al., 2008). The balance of stream power and erosional resistance define a relationship in which streams respond to tectonically induced changes in topography by either incising into or diverting around growing structures (Bull, 1991). Erosional resistance is influenced by surface or rock uplift, lithologic characteristics, and sedimentation (Burbank et al., 1996; Sklar and Dietrich, 1998; Humphrey and Konrad, 2000); slope and drainage area determine stream power (Gilbert, 1877; Howard and Kerby, 1983; Seidl and Dietrich, 1992). If erosional resistance is greater than incision, streams will be defeated and deflected along the active fold. In this process the drainage area will increase until the stream power overweighs erosional resistance and the stream

* Corresponding author at: Department of Earth and Planetary Science, McGill University, Montreal, Quebec, Canada H3A 2A7.
E-mail address: benjamin.melosh@mail.mcgill.ca (B.L. Melosh).

0169-555X/$ – see front matter © 2013 Elsevier B.V. All rights reserved.
http://dx.doi.org/10.1016/j.geomorph.2012.12.027

incises a new channel across the active structure. In this paper we refer to stream diversion in the sense of a tectonic diversion rather than a non-tectonically caused diversion such as stream capture and rerouting (e.g. Bishop, 1995).

Defeated streams leave a lasting imprint on the landscape in the form of geomorphic paleochannels. The topographic breaks in fold profiles formed where paleochannels and active streams traverse the axial hinge are termed "wind gaps" and "water gaps", respectively (Burbank et al., 1996, 1999; Keller and Pinter, 2002). We note that the term "wind gap" has been applied in situations where headward incision causes the abandonment of channels (Bishop, 1995); we use this term as described above in the sense of Keller and Pinter (2002). These geomorphic features provide valuable strain markers when unraveling the Quaternary tectonic history of a fold belt.

Previous studies have used stream and paleochannel patterns as geomorphic tools to identify folds (e.g. Gupta, 1997; Boudiaf et al., 1998), determine fold propagation direction (Jackson et al., 1996; Keller et al., 1998, 1999), determine fold growth rates (Medwedeff, 1992), differentiate between fault tip propagation and slip accumulation (e.g. Amos et al., 2010), determine fault slip rates (e.g. Sieh and Jahns, 1984), and assess seismic hazard in fold belts (e.g. Keller and Gurrola, 2000). Keller et al. (1999) mapped paleochannels on the backlimb of western Mission Ridge anticline in Santa Barbara, California; they recognized that drainage pattern, drainage density, and backlimb rotation all indicate a westward propagation direction. But they did not expand the study past this one anticline.

Geomorphic indices of active tectonics developed by Bull and McFadden (1977) are a set of tools that utilize landscape morphology to quantitatively assess landscape evolution in active tectonic settings. Some of these metrics include valley width to height ratio, mountain front sinuosity and drainage density (described below). For example, Silva et al. (2003) used geomorphic indices to test the morphologic properties of different styles of faulting and assign a tectonic activity class to different mountain fronts. Azor et al. (2002) applied geomorphic indices to a hanging wall anticline on a reactivated normal fault in southern California, and determined that the morphology of the fold was controlled by a decrease in fault slip rather than propagation of the fault tip. A detailed analysis using geomorphic indices has not been applied in the Santa Barbara Fold Belt (SBFB).

Many orogenic systems involve complex deformation patterns and previous geomorphic studies focus mostly on individual structures. The SBFB contains two coevally interfering sets of active structures oriented roughly 30° from each other. In this paper we use drainage patterns, the strain markers of paleochannels and alluvial fans, as well as geomorphic indices of active tectonics to determine stream incision, fold propagation direction and the relative timing of structural overprinting in the SBFB. We test the hypotheses that: 1) incision and uplift are approximately equal and thus the landscape is in steady state; 2) folds in the SBFB generally propagate westward; and 3) east–west oriented folds are the most recent manifestation of north–south shortening in a clockwise rotating micro-block.

1.2. Tectonic geomorphology background of the SBFB and field area

The SBFB is a zone of continental shortening in an urban setting with a uniform climate and well-mapped geology where we can perform a detailed geomorphic analysis to understand Quaternary tectonic evolution. The geology comprises steeply dipping sandstone and shale striking sub-parallel to the Santa Ynez Mountains and perpendicular to the streams draining to the Pacific Ocean (Dibblee, 1966; Minor et al., 2009). Average annual precipitation increases two fold from the coast to the crest of the Santa Ynez Mountains from 43 cm/yr to 79 cm/yr (Gibbs, 1990). For a given elevation, precipitation is uniform across the range; drainages are of similar size and elevation.

The field area is located on the coastal piedmont around Santa Barbara, California between the towns of Ellwood and Montecito, approximately 145 km (90 miles) north of Los Angeles (Fig. 1). The SBFB is structurally bound by two left lateral faults: the Santa Ynez fault to the north and the Santa Cruz Island fault to the south (Fig. 1), and is a westward continuation of the Ventura Fold belt (Gurrola, 2006). Within the field area the SBFB consists of a series of topographic ridges and valleys that are the surface expression of anticline-syncline pairs resulting from reverse faulting associated with crustal shortening (Yeats, 1986; Keller and Gurrola, 2000). These folds have either a southeast–northwest or an east–west orientation, where east–west folds truncate southeast-northwest folds.

The overlapping deformation pattern within the SBFB is a product of a complex tectonic history. Paleomagnetic data show that since early Miocene time the western Transverse Ranges (including the field area) have rotated as much as 100° in a clockwise direction (Hornafius et al., 1986). Luyendyk et al. (1980) propose a geometric model by which continued dextral shear along the San Andreas boundary is accommodated by sinistral slip and clockwise rotation of the western Transverse Ranges. This requires that the SBFB first experienced extension and then compression while undergoing continued clockwise rotation (see palinspastic reconstructions of Hornafius et al. (1986) and the "Southern California Breakup and Paleomagnetic Vector Rotations, 20 Ma to Present" animation by Tanya Atwater). The later compressional phase of deformation was enhanced due to the formation of the Big Bend in the San Andreas system during the late Neogene (Crowell, 1979). Recent GPS studies reveal continued clockwise rotation of the region (Meade and Hager, 2005).

1.2.1. Faults

The Mission Ridge fault system, which dominates the onshore portions of the SBFB, extends about 70 km from Ojai to Ellwood where it continues offshore. If the entire length of the fault were to rupture in one event it could create a M7.2+ earthquake (Wells and Coppersmith, 1994). Within the SBFB the Mission Ridge fault system is characterized by three predominant styles of active faults. These are east–west trending blind reverse faults, southeast–northwest trending blind reverse faults, and north–south lateral tear faults (Keller and Gurrola, 2000; Gurrola, 2006; Minor et al., 2009). Blind reverse faults dip 60–70° to the south (Gurrola, 2006) and associated hanging wall anticlines are north vergent. East–west faults include the More Ranch fault; southeast–northwest faults include the Mission Ridge fault, Mesa fault, Lavigia fault, and the San Jose fault; tear faults do not significantly divert stream channels, and are not included as part of this study (cf. Fig. 1). More Ranch fault develops a northeast–southwest orientation between Hope Ranch and the city of Santa Barbara; we include this in our results and discussions of east–west structures because the overall strike of the fault is east–west (see geologic map of Minor et al., 2009).

1.2.2. Previous work: geochronology, uplift rates and mapping

Previous workers have collected and analyzed a suite of geochronologic data in the area that provide us a powerful tool when evaluating the evolution of the SBFB. The techniques used include cosmogenic ^{21}Ne exposure dating, optically stimulated luminescence and uranium series analysis. Zepeda (1987) estimated the age of the alluvial fan deposit to the north of the Goleta Valley anticline, labeled Qf2b in this study, to be between 70 and 100 ka. Subsequently Keller and Gurrola (2000) used optically stimulated luminescence (OSL) and uranium-series analysis on marine terrace sands and shells to estimate the ages of marine terraces and uplift rates of the SBFB. OSL samples, within the field area, were collected from four marine terrace locations: the Cemetery anticline terrace, the Mesa terrace, the Hope Ranch terrace and the Campus terrace (Gurrola, 2006). Samples for U-series analysis were collected at the Mesa terrace and the Campus terrace. Landis et al. (2002), performed a series of six

Please cite this article as: Melosh, B.L., Keller, E.A., Effects of active folding and reverse faulting on stream channel evolution, Santa Barbara Fold Belt, California, Geomorphology (2013), http://dx.doi.org/10.1016/j.geomorph.2012.12.027

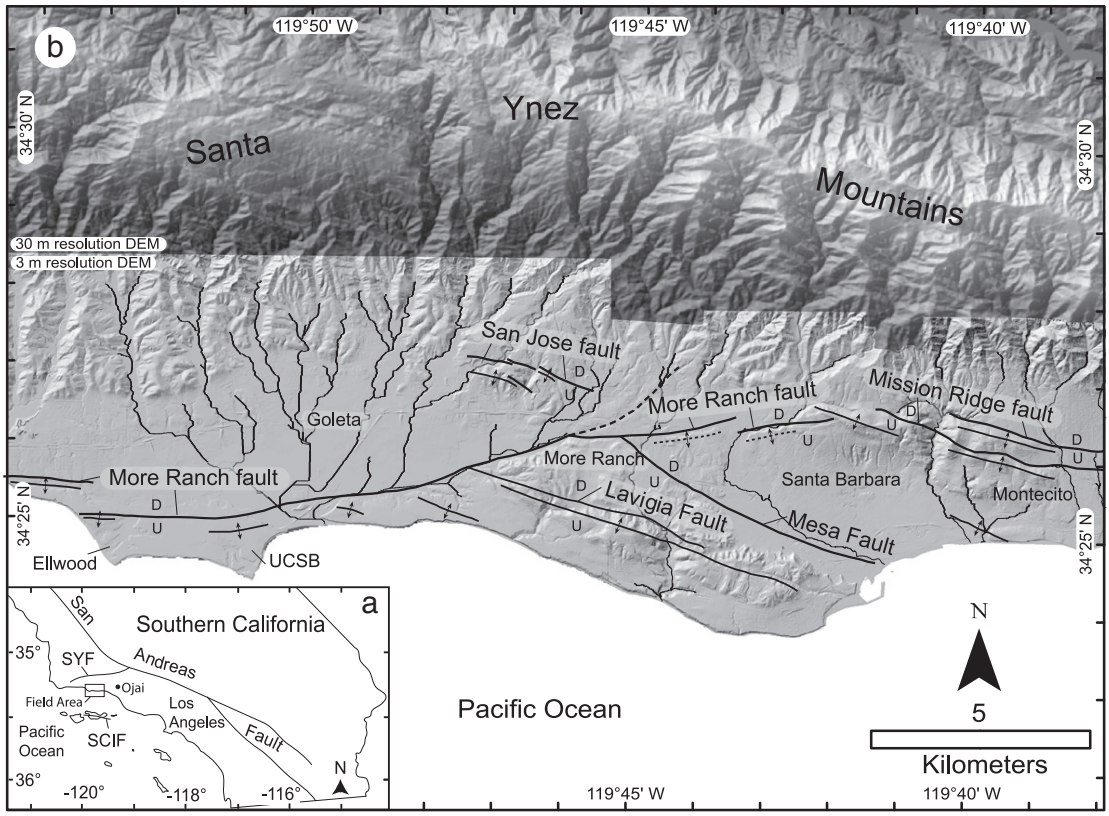

Fig. 1. a) Location of the field area in relation to the San Andreas Fault, the Santa Ynez fault (SYF), the Santa Cruz Island fault (SCIF) and Los Angeles. The field area is located within the Santa Barbara Fold Belt. b) Hillshade of the field area from 3 and 30 meter resolution data, the 30 m hillshade is partially transparent and overlain on the DEM. Geographic landmarks include, from east to west: Montecito, Santa Barbara, More Ranch, Goleta, UCSB campus, and Ellwood. The field area is the coastal piedmont between the Santa Ynez Mountains to the north and the Pacific Ocean.

cosmogenic ^{21}Ne exposure dates on the Rattlesnake alluvial fan, Qf3 in this study, and calculated ages between 93 and 139 ka. Sample locations are mapped in Plate 4 of Gurrola (2006). We correlate (using arguments of Bull, 1991) deposition of the fan with an aggradational event during the Eemian (~125 ka). This correlation is based on the fact the Qf3 is the highest alluvial fan in the field area, located at a maximum elevation of 350 m, at a distance of 5.2 km from the coast. Assuming modern uplift rates (1.2–1.3 m/ka) (Keller and Gurrola, 2000) were constant over the last 125 ka and adding 5 m for the relative change in sea level in southern California (Muhs et al., 2012), the Eemian shoreline occurred at a modern elevation of ~125–135 m.

Keller and Gurrola (2000) and Gurrola et al. (in review) calculate uplift rates in the SBFB that range from 0.4 to 1.9 m/ka. Uplift rates are lowest in the east near the town of Montecito and are greatest in the west near the UC Santa Barbara campus. Because these marine terrace surfaces are young and not highly dissected the uplift rates approximate a surficial uplift with respect to the geoid (England and Molnar, 1990). England and Molnar (1990) distinguish between three different kinds of uplift: surface uplift with respect to the geoid, uplift of rocks with respect to the geoid, and uplift of rocks with respect to the surface (exhumation). We present these terms here as we refer to them in the following text.

Previous work in the SBFB also includes detailed geologic and geomorphic mapping. Geologic maps of the central Santa Ynez Mountains (1:62,500), and the Santa Barbara and Goleta quadrangles (1:24,000) (Dibblee, 1966, 1986, 1987) paved the way for the more recent geologic map of the Santa Barbara coastal plain by Minor et al. (2009) (1:25,000). Original mapping by Dibblee (1966, 1986, 1987) has consistently been proven accurate (Gurrola, personal communication). Lastly, Keller and Gurrola (2000) and Gurrola (2006) created detail geomorphic maps of marine terraces and alluvial fans in the SBFB. These maps in combination with geochronologic data and uplift rates provide a foundation for this investigation.

2. Methods

2.1. Geomorphic mapping and topographic analysis

In this study we utilize a digital elevation model (DEM) compiled from total station survey data provided by Santa Barbara County. Elevation data were interpolated to create a raster dataset; therefore, this DEM does not include vegetation or buildings that might obscure underlying landforms. The lateral and vertical resolutions are 3 and 0.6 m, respectively. This high-resolution DEM and associated hillshade image is used because it allows for easy identification and mapping of geomorphic features in an urban area with access restrictions. Roads and freeways, however, are included in the DEM, and can be seen in the hillshade images presented below. Areas where base station data was sparse present a lower spatial resolution. To avoid error in these areas, hand-held GPS surveys were performed with Trimble GeoXH units. With two GPS units, one acting as a base station, 20 cm vertical accuracy can be achieved along structures and geomorphic features of interest.

We expand upon previous work using this DEM to map paleochannels, measure incision amounts, measure diversion distances, measure uplift amounts, and calculate geomorphic indices of active tectonics. Combined with chronological information we calculate rates of stream incision, minimum uplift at western Mission Ridge anticline and the Mesa fault, and the stream diversion index. To draw active streams we use an ArcInfo script that calculates the flow path through

Please cite this article as: Melosh, B.L., Keller, E.A., Effects of active folding and reverse faulting on stream channel evolution, Santa Barbara Fold Belt, California, Geomorphology (2013), http://dx.doi.org/10.1016/j.geomorph.2012.12.027

a basin by assessing pixel elevations and assigning streams to topographically low points with a D8 algorithm.

2.2. Incision and minimum uplift rates

Mean stream incision rates are calculated at four locations: Arroyo Burro Creek, Hope Ranch Creek, Rattlesnake Creek and Sycamore Creek (Fig. 2). These creeks were chosen because they incise through dated geomorphic surfaces. Ten cross-channel profiles were extracted from the DEM where the creeks have incised though previously dated surfaces; the incision rate is determined by dividing the vertical incision distance by the age of the surface.

Minimum uplift rates are estimated for the western Mission Ridge anticline and the Mesa fault. Western Mission Ridge anticline folds a previously dated alluvial fan (Landis et al., 2002; Gurrola, 2006). Mean vertical displacement from a presumed depositional surface is measured by extracting topographic profiles of the alluvial fan across the axial trace of western Mission Ridge anticline (Fig. 3). This distance is then divided by the fan exposure age to estimate the minimum uplift rate. This uplift is a minimum value because we do not have a way to constrain the position of the alluvial fan relative to the geoid during deposition. Uplift on the Mesa fault is estimated using abandoned paleochannels as strain makers. Three of the four paleochannels on the backlimb (numbered 2–4 in Fig. 3) are oriented perpendicular to the Mesa fault; the remaining paleochannel (numbered 1) is oriented fault sub-parallel. Paleochannel 1 is not as sensitive to movement of the Mesa fault because it is oriented sub-parallel to the fault at a greater distance away and therefore we assume it maintains its original morphology. As paleochannels 2 through 4 approach the Mesa fault they diverge vertically from paleochannel 1. The elevation difference between paleochannels 1 and 2–4 divided by the approximate age of the paleochannels (the time at which streams would have their original morphology) provides an estimate of the minimum uplift rate of the Mesa fault.

2.3. Geomorphic indices of relative tectonic activity

Geomorphic indices are produced to estimate relative tectonic activity. These indices are measures of the balance between erosional and tectonic forces, and work under the assumption of uniform climate and lithology.

Valley width to height ratio (Vf) is the ratio of valley floor width to mean relief as measured on a cross channel elevation profile and is described by the following equation:

$$Vf = 2Vfw/[(Eld–Esc) + (Erd–Esc)], \quad (1)$$

Where Vf is the valley floor width to height ratio; Vfw is the valley floor width; Eld and Erd are elevations on the left and right side of the valley divides, respectively; and Esc is the elevation of the valley floor (Bull, 1977, 1978; Azor et al., 2002; Keller and Pinter, 2002; Burbank and Anderson, 2012). Landscapes experiencing active uplift commonly have deep valleys with actively incising streams, reflected in a low Vf value. The opposite is observed where streams cut wide valley floors associated with low uplift. Higher values of Vf, therefore, indicate a lesser degree of tectonic activity.

Mountain front sinuosity (Smf) is the ratio of length of the mountain front, measured along the ground at the abrupt change in slope between the mountain front and the adjacent low-relief region (Lmf), to the straight-line length of the mountain front ignoring bends (Ls) (Bull, 1977, 1978; Keller and Pinter, 2002):

$$Smf = Lmf/Ls. \quad (2)$$

Smf is measured on the fore and back limbs of anticlines. Erosion tends to create a sinuous mountain front with a high Smf value, while tectonic uplift tends to form a straight mountain front with a low Smf value (Keller and Pinter, 2002).

Drainage density (Dd) is the ratio of drainage length versus catchment area in units of km/km^2 (Azor et al., 2002; Keller and Pinter, 2002). Values of Dd depend on the degree to which erosion or drainage development has dissected a structural landform. Drainage systems are more extensively developed on older landforms that have been exposed on the surface for a relatively long time and therefore have greater values of Dd. Areas experiencing the most recent tectonic activity will have lower values of Dd (Keller and Pinter, 2002). Dd is calculated by summing the length of all stream channels and drainages in sections of each fold and dividing by the area.

Stream diversion is an index presented here for the first time; it is used to help categorize relative duration of a folds' surface exposure from which we can infer tectonic activity. This index is calculated by dividing the distance of stream diversion by the time of diversion. Distance of stream diversion is a measure between abandoned paleochannel and active channel measured along strike with the structure that caused the diversion. To make this measurement we first identify what streams occupied specific paleochannels. The time of diversion is constrained by the spatial relationships of dated surfaces to paleochannel position and incision. For example, a paleochannel incised into a 47 ka marine terrace must have been abandoned less than 47 ka. Fold growth is the process causing stream diversion to occur, however during diversion a stream will not follow the fold expression perfectly and therefore the stream diversion index cannot be used to measure fold growth. Finally, topographic profiles of each anticline, drawn along the axial trace, highlight wind gaps, and water gaps providing a qualitative assessment of fold dissection and relief.

3. Results

The results are presented in order of how the methods were applied. Beginning with incision rates we test the hypothesis of steady state. Geomorphic paleochannel maps, diversion distances, and geomorphic indices are presented next, to test the hypotheses of westward fold growth and the overprinting relationship of east–west oriented structures on southeast-northwest structures. Each fold studied is the subject of its own subsection and catagoried by orientation (east–west or southeast-northwest) in the presentation of the data.

3.1. Incision rates

The incision rates at Arroyo Burro Creek and Hope Ranch Creek are 0.4 ± 0.1 m/ka. These creeks incise through marine terraces formed during oxygen isotope stages (OIS) 3, 5 and 7 (Keller and Gurrola, 2000), and record minimum incision rates due to an unknown amount of alluvial fill and differential incision, respectively. Differential incision refers to a varying incision history caused by channel diversion events and subsequent changes in drainage area. These measurements were taken in the hanging wall of the Mesa and Lavigia faults.

Bedrock channels of Rattlesnake and Sycamore Creeks both incise through Qf3, a 93–139 ka-old alluvial fan (Dibblee, 1966; Landis et al., 2002; Gurrola, 2006; Minor et al., 2009). The incision rate at Rattlesnake Creek, measured in the footwall of the Mission Ridge fault, is 0.6 ± 0.1 m/ka. Incision of Sycamore Creek in the hanging wall of the Mission Ridge fault, near the axial trace of Mission Ridge anticline is 1.2 ± 0.04 m/ka (Fig. 2).

3.2. Mission Ridge anticline

Mission Ridge anticline changes orientation between its eastern and western portions. The eastern portion of Mission Ridge anticline

Please cite this article as: Melosh, B.L., Keller, E.A., Effects of active folding and reverse faulting on stream channel evolution, Santa Barbara Fold Belt, California, Geomorphology (2013), http://dx.doi.org/10.1016/j.geomorph.2012.12.027

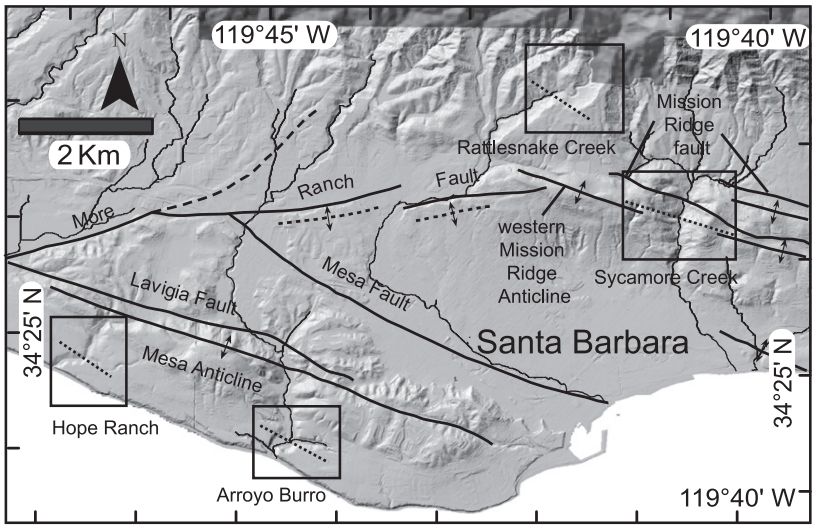

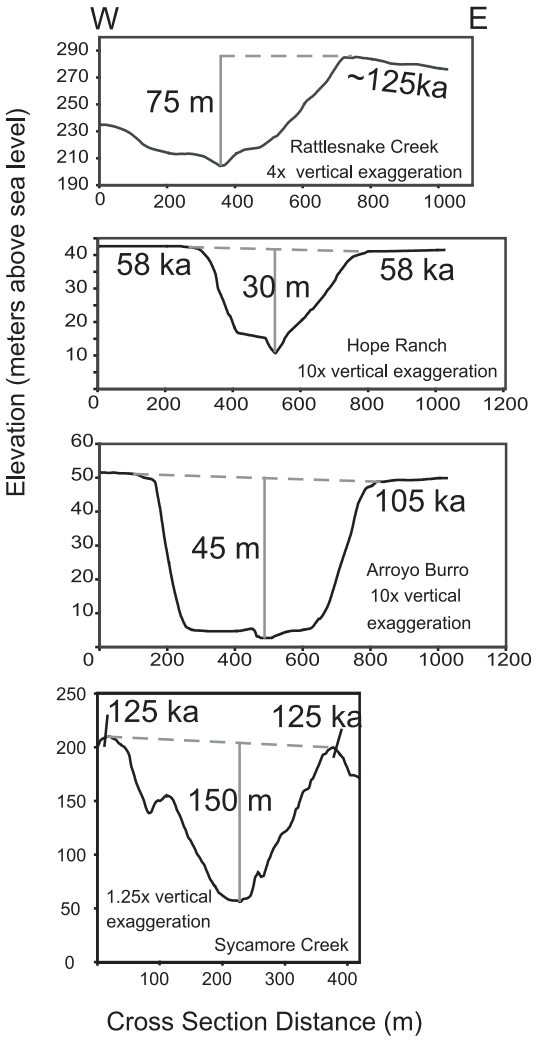

Fig. 2. Hillshade map of the SBFB showing locations where stream incision rates were calculated (boxed), black dashed bars represent cross channel profile lines. Note: ten cross-channel profiles were measured along each reach. Representative cross-channel profiles of Rattlesnake, Hope Ranch, Arroyo Burro and Sycamore Creeks are shown below map.

is oriented southeast–northwest and the westernmost segment is oriented east–west (slightly northeast–southwest). This change in geometry is caused by the bifurcation of More Ranch fault from Mission Ridge fault near downtown Santa Barbara. Deformation at the westernmost portion of the Mission Ridge anticline is attributed to the More Ranch fault. Based on the deformation of younger

Please cite this article as: Melosh, B.L., Keller, E.A., Effects of active folding and reverse faulting on stream channel evolution, Santa Barbara Fold Belt, California, Geomorphology (2013), http://dx.doi.org/10.1016/j.geomorph.2012.12.027

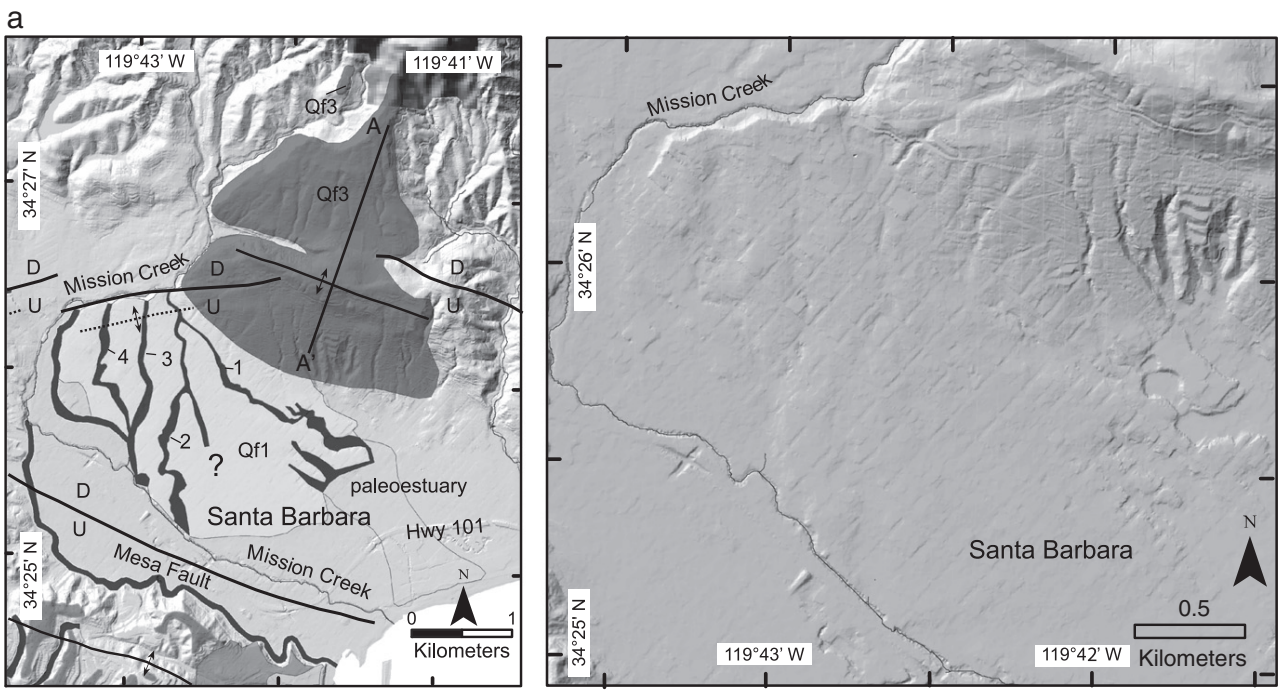

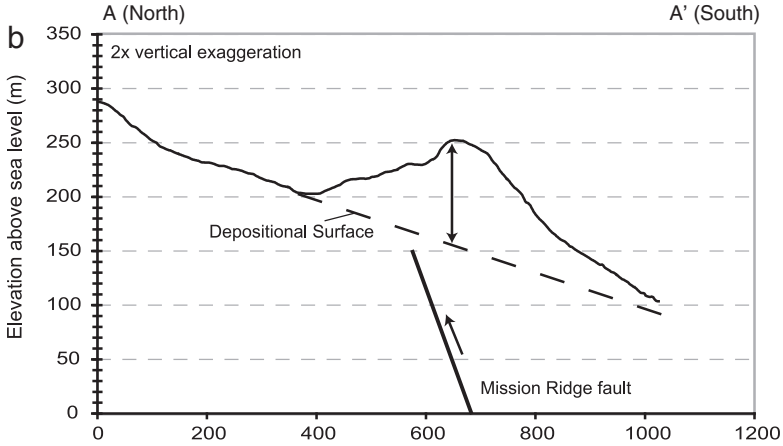

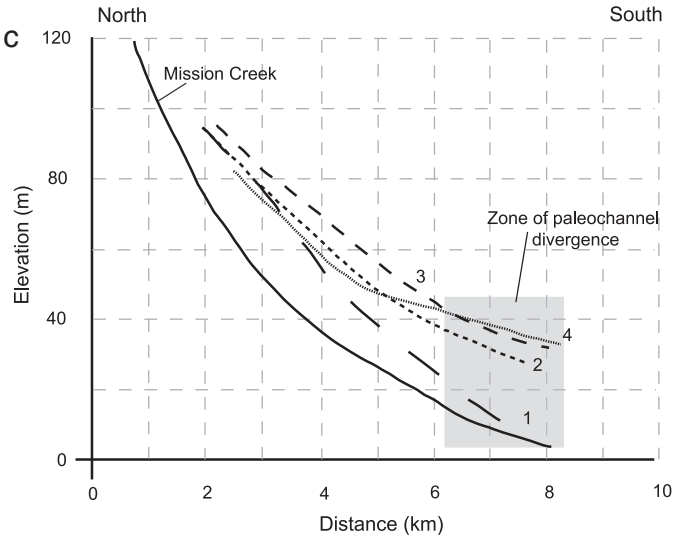

Please cite this article as: Melosh, B.L., Keller, E.A., Effects of active folding and reverse faulting on stream channel evolution, Santa Barbara Fold Belt, California, Geomorphology (2013), http://dx.doi.org/10.1016/j.geomorph.2012.12.027

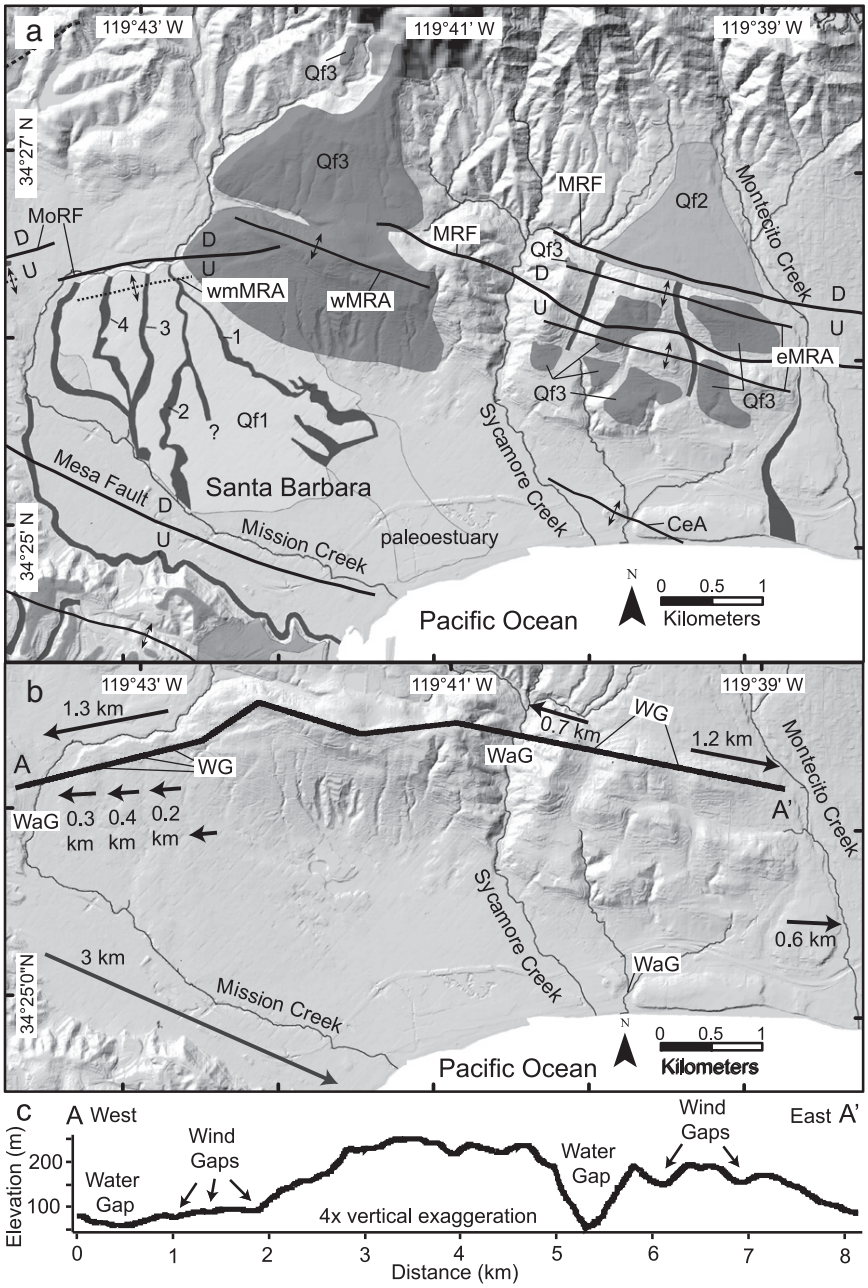

Fig. 4. (a) Geomorphic map of Mission Ridge anticline. Structures, marine terraces and alluvial fan surfaces are modified after Gurrola (2006). Paleochannels, shown in black, are mapped as part of this investigation. Anticlines include: eastern Mission Ridge anticline (eMRA), western Mission Ridge anticline (wMRA), westernmost Mission Ridge anticline (wmMRA), and the Cemetery anticline (CeA). Faults include: the Mission Ridge fault (MRF), the More Ranch fault (MoRF), and the Mesa fault. (b) Map demonstrating paleochannel diversion locations, directions, and approximate magnitudes, marked by arrow location, direction, and length, respectively. Important geomorphic features include: wind gaps (WG), water gaps (WaG), and divergence locations (Div). Cross-section line (A–A′) marks where the topographic profile, shown in (c). (c) Topographic profile between A and A′, wind and water gaps are marked.

material and lesser topographic expression, More Ranch fault is the younger of the two faults.

3.2.1. Northwest–southeast oriented sections

Mission Ridge is divided for purpose of discussion into three segments: eastern Mission Ridge, western Mission Ridge, and westernmost Mission Ridge (Fig. 4). Eastern Mission Ridge, located in the eastern portion of the field area, is formed by a hanging wall anticline above the Mission Ridge fault. It is oriented southeast-northwest. At this location the fault is splayed into a northern and southern segment and the anticline is well dissected, with two prominent wind gaps (Fig. 4). The paleochannel network around the eastern Mission Ridge anticline shows evidence of three channel diversion events (Fig. 4b); a tributary of Sycamore Creek was diverted

Fig. 3. (a) Geomorphic map of Mission Ridge and Santa Barbara city area and hillshade image showing geomorphic paleochannel positions. The black bar represents locations where long fan profiles are drawn. Paleochannels labeled 1 through 4 are used in the calculation for uplift along the Mesa fault. (b) Topographic profile measured down alluvial fan Qf3, perpendicular to western Mission Ridge anticline, demonstrating how uplift rate of Mission Ridge anticline is calculated. Note: a total of ten profiles were measured. (c) Long channel profiles of Mission Creek and paleochannels 1 though 4. As paleochannels 2 through 4 approach the Mesa fault they diverge in elevation from paleochannel 1, oriented parallel to fault. The mean elevation divergence divided by the age of alluvial fan Qf1 is the minimum uplift rate for the Mesa fault.

Please cite this article as: Melosh, B.L., Keller, E.A., Effects of active folding and reverse faulting on stream channel evolution, Santa Barbara Fold Belt, California, Geomorphology (2013), http://dx.doi.org/10.1016/j.geomorph.2012.12.027

west and Montecito Creek was diverted east two times. The Sycamore Creek diversion and the first Montecito Creek diversion occurred between 60 and 139 ka as suggested by the 60–100 ka age of an alluvial fan (Qf2) buttressed against the forelimb of east Mission Ridge anticline and the older alluvial fan (Qf3) (93–139 ka) dissected along the fold crest (Fig. 4a). Total stream displacement distances are 0.7 and 1.2 km with diversion indices of 20–9 and 12–5 m/ka, respectively. The second diversion of Montecito Creek, a 0.6 km eastward diversion, occurred after 60 ka. Eastern Mission Ridge anticline exhibits a decrease in elevation and surface dissection toward the east, as observed on the topographic profile (Fig. 4c).

Western Mission Ridge anticline (the central segment) (Fig. 4) occurs in the hanging wall of Mission Ridge fault and is oriented southeast–northwest. This section displays little incision and contains no paleochannels. The alluvial fan Qf3 (93–139 ka) (Landis et al., 2002; Gurrola, 2006) is folded over this part of the anticline. Average vertical tectonic relief is 92 m, and a minimum uplift rate of 0.8 ± 0.1 m/ka is estimated (Fig. 3b).

3.2.2. East–west oriented section

The westernmost Mission Ridge anticline occurs in the hanging wall of the More Ranch fault, contains 3 wind gaps and 4 paleochannels on the back limb and diverts Mission Creek 1.3 km to the west (Fig. 4b). This segment uplifts a latest Pleistocene, 60–70 ka, alluvial fan (Qf1) (Keller et al., 1999; Gurrola, 2006), and has a diversion index of >22 m/ka. As paleochannels (2–4 in Fig. 4a) approach the Mesa fault they diverge vertically, by an average of 21 m, from paleochannel 1. The vertical divergence divided by the age of the surface the paleochannels incise, Qf1 (60–70 ka), is the minimum uplift rate of the Mesa fault at 0.3–0.4 m/ka (Fig. 4c).

Values of Smf and Dd at Mission Ridge anticline, including all three sections discussed above (Fig. 5), are consistently lower in the west than in the east and values calculated for the entire anticline are relatively low when compared with both east–west and southeast–northwest structures (Table 1). The value of Vf, calculated for the entire anticline, is the minimum value found in the study.

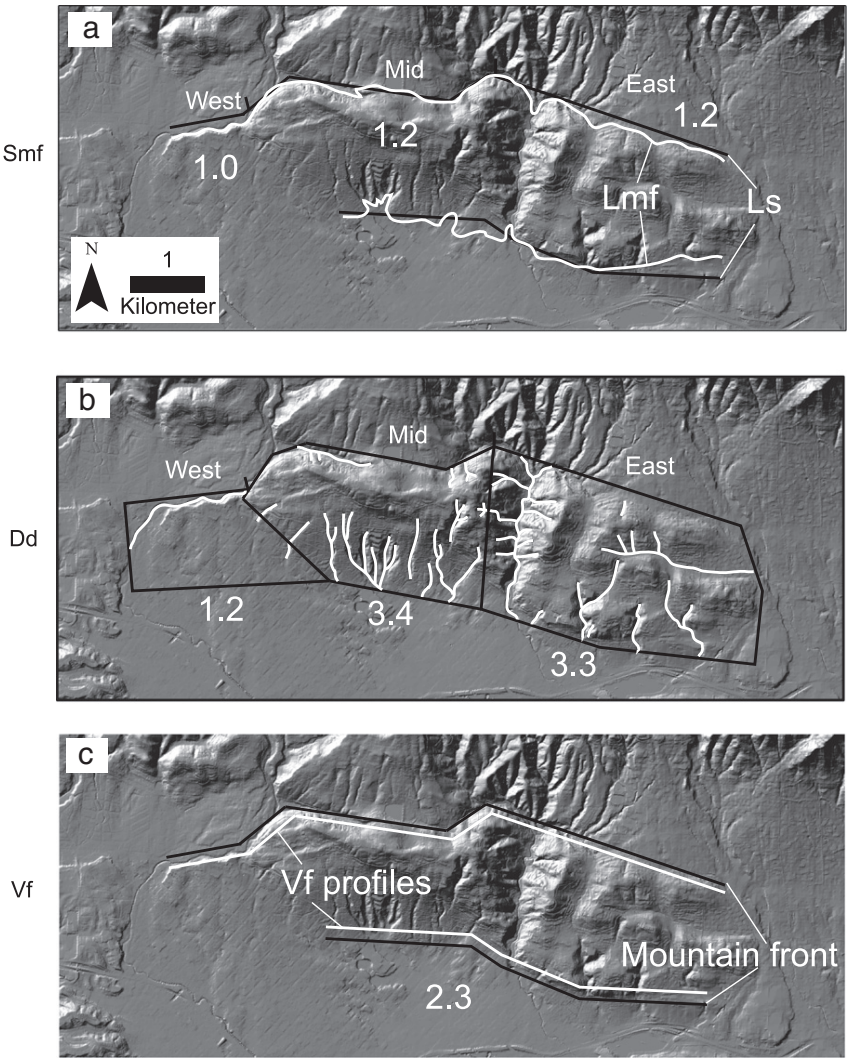

Fig. 5. (a) Map demonstrating how values of mountain front sinuosity were calculated at Mission Ridge anticline. White lines are sinuous mountain front lengths and black lines are straight-line mountain front lengths. The fold is divided into west, middle and east sections to test for variations in mountain front sinuosity along strike. Values of Smf are shown for each section. (b) Map demonstrating how values of drainage density were calculated. Boxes represent drainage area in eastern, middle and western segments, white lines represent drainages. Values of Dd are shown for each section. (c) Map demonstrating how valley width to height ratios are calculated. Black lines mark mountain fronts and white lines are locations, 0.1 km from the mountain front, where valley width to height is measured. Value of Vf is shown.

Please cite this article as: Melosh, B.L., Keller, E.A., Effects of active folding and reverse faulting on stream channel evolution, Santa Barbara Fold Belt, California, Geomorphology (2013), http://dx.doi.org/10.1016/j.geomorph.2012.12.027

Table 1
Numerical values of valley width to height ratio (Vf), mountain front sinuosity (Smf), and drainage density (Dd) for all anticlines studied, Smf and Dd are subdivided into east, middle and west sections. Vf values were not measured in individual segments due to lack of viable locations. * indicates the east–west oriented portion of the Mission Ridge anticline.

Anticline	Orientation	Valley width to height ratio (Vf)	Mountain front sinuosity (Smf)			Drainage density (km/km^2) (Dd)		
Hope Ranch–Ellwood	East–West	3.0	1.1			1.9		
			West	Mid	East	West	Mid	East
			1.1	1.1	1.2	0.5	2.2	6.6
Mission Ridge	East–West and Southeast–Northwest	2.3	1.3			2.7		
			*West	Mid	East	*West	Mid	East
			1.0	1.2	1.2	1.2	3.4	3.3
Mesa	Southeast–Northwest	4.6	1.2			2.8		
			West	Mid	East	West	Mid	East
			NA	1.2	1.3	3.3	3.2	2.1
Goleta Valley	Southeast–Northwest	5.3	1.7			4.5		
			West		East	West		East
			1.9		1.6	5.1		3.9

3.3. The Mesa anticline: southeast–northwest oriented

The Mesa anticline is a southeast–northwest oriented structure (Fig. 6a). North–south oriented paleochannels on the Mesa anticline, numbered 1 and 2 in Fig. 6a, record the former location of Mission Creek, which was diverted east a total of 3 km (Fig. 6b). Paleochannels 1 and 2 are incised through the marine oxygen isotope stage (MIS) 7 (~200 ka) marine terrace, but not the MIS 5 marine terrace. Therefore, diversion of Mission Creek at this location occurred between 200 and 125 ka, with a diversion index of 15–24 m/ka. Mission Creek has largely removed the forelimb of the Mesa anticline, as evidenced by large meander scars and the distance between the Mesa fault and the topography of the Mesa anticline. The paleochannel labeled HR in Fig. 6a records the former position of Atascadero Creek, which was diverted due to movement along the More Ranch fault; this diversion is presented in the following Hope Ranch to Ellwood Anticlinorium section.

The topographic profile of the Mesa anticline displays high relief, two wind gaps, and one water gap (Fig. 6c). Values of Smf do not show a meaningful trend because we could not collect values at the western portion of the anticline due to the lack of a definable mountain front (Fig. 7). The value of Smf for the anticline as a whole is low. Values of Dd decrease to the east along the Mesa anticline with an overall value that is higher than east–west oriented structures. The Value of Vf is also higher than east–west oriented structures (Table 1).

3.4. Goleta Valley anticline: southeast–northwest oriented

The Goleta Valley anticline is a southeast–northwest trending fold in the hanging wall of the San Jose fault (Fig. 8a). The fold deforms alluvial fan deposits Qf2b (70–100 ka) (Zepeda, 1987), as well as marine terrace deposits of probable MIS 5 (Gurrola, personal communication). The evolution of the Goleta Valley anticline drainage system is indicative of both eastward and westward fold propagation. Stream diversions include a 0.4 km westward diversion of San Antonio Creek and a 0.5 km eastward diversion of a tributary to Atascadero Creek (Fig. 8b). Both diversions occurred after the 70–100 ka-year old alluvial fan was deposited and therefore the diversion index is 5–7 m/ka.

A topographic profile of the Goleta Valley anticline (Fig. 8c) displays a highly incised morphology, two wind gaps and two water gaps. The Goleta Valley anticline has the highest values of Vf, Smf and Dd found during this investigation (Fig. 9, Table 1). Due to the limited size of the Goleta Valley anticline only east and west sections were analyzed.

3.5. Hope Ranch to Ellwood anticlinorium: east–west oriented

The east–west oriented Hope Ranch to Ellwood anticlinorium occurs in the hanging wall of the More Ranch fault. There are five paleochannels, labeled HR, MM and numbered 1–3 in Fig. 10a. The largest stream diversion found in this investigation occurs along the Hope Ranch to Ellwood anticlinorium where Atascadero Creek is diverted 6.7 km to the west. This includes two diversions of 5.6 km and 1.1 km, occurring <47 ka and between 43.5 and 6.5 ka, respectively (Fig. 10b). The stream diversion index is 25–183 m/ka. Paleochannels HR and MM record the positions of Atascadero Creek throughout the diversion history. The timing of the first diversion was constrained by the age of the youngest incised marine terrace at Hope Ranch. To constrain the second diversion timing we performed two differential GPS surveys using hand held Trimble GeoXH units. The first survey was measured down the length of the paleochannel at the lowest point; the second survey was taken adjacent the paleochannel, traversing the folded marine terrace. The average difference in elevation between these surveys is 3.9 m. This elevation difference, divided by the average calculated incision rates, 0.4–1.2 m/ka, shows that incision persisted for 9.8–3.3 ka (Fig. 11a). This time subtracted from the age of the incised surface, 47 ± 0.5 ka (Keller and Gurrola, 2000), provides a diversion time of 37.2–43.7 ka. We also calculated diversion timings by another method. The difference in elevation between the uplifted, hanging wall paleochannel and the adjacent footwall, divided by the marine terrace uplift rate from Keller and Gurrola (2000) provides a diversion time of 5 ± 2 ka (Fig. 11b). This value is a minimum due to an unknown amount of fill on the footwall block.

The paleochannel at UCSB, number 1 (cf. Fig. 10a), on the western portion of Hope Ranch to Ellwood anticlinorium is oriented north–south (Fig. 11c). The paleochannel displays several incised meander bend cutoffs in a 47 ± 0.5 ka marine terrace (Keller and Gurrola, 2000) and an eastward diversion of 1.3 km in response to uplift on the More Ranch fault sometime after the formation of the marine terrace and sometime before 5 ± 2 ka. Again, minimum diversion timing was calculated based on the elevation difference between uplifted paleochannel and footwall blocks (Fig. 11b). The stream diversion index is 260 m/ka.

Hope Ranch–Ellwood anticlinorium has the lowest Vf, Smf and Dd values found during this study (Fig. 12). Values of Dd show a strong decreasing trend toward the west although values of Smf stay nearly constant, dropping slightly between eastern and middle sections (Table 1). The topographic profile displays one wind gap, and one water gap and shows a decrease in dissection and relief toward the west (cf. Fig. 10c).

4. Discussion

The SBFB is tectonically complicated and currently experiencing shortening and clockwise rotation (Meade and Hager, 2005). We hypothesize that as the Santa Barbara micro-block continues to rotate, the structures accommodating shortening are rotated until a new

Please cite this article as: Melosh, B.L., Keller, E.A., Effects of active folding and reverse faulting on stream channel evolution, Santa Barbara Fold Belt, California, Geomorphology (2013), http://dx.doi.org/10.1016/j.geomorph.2012.12.027

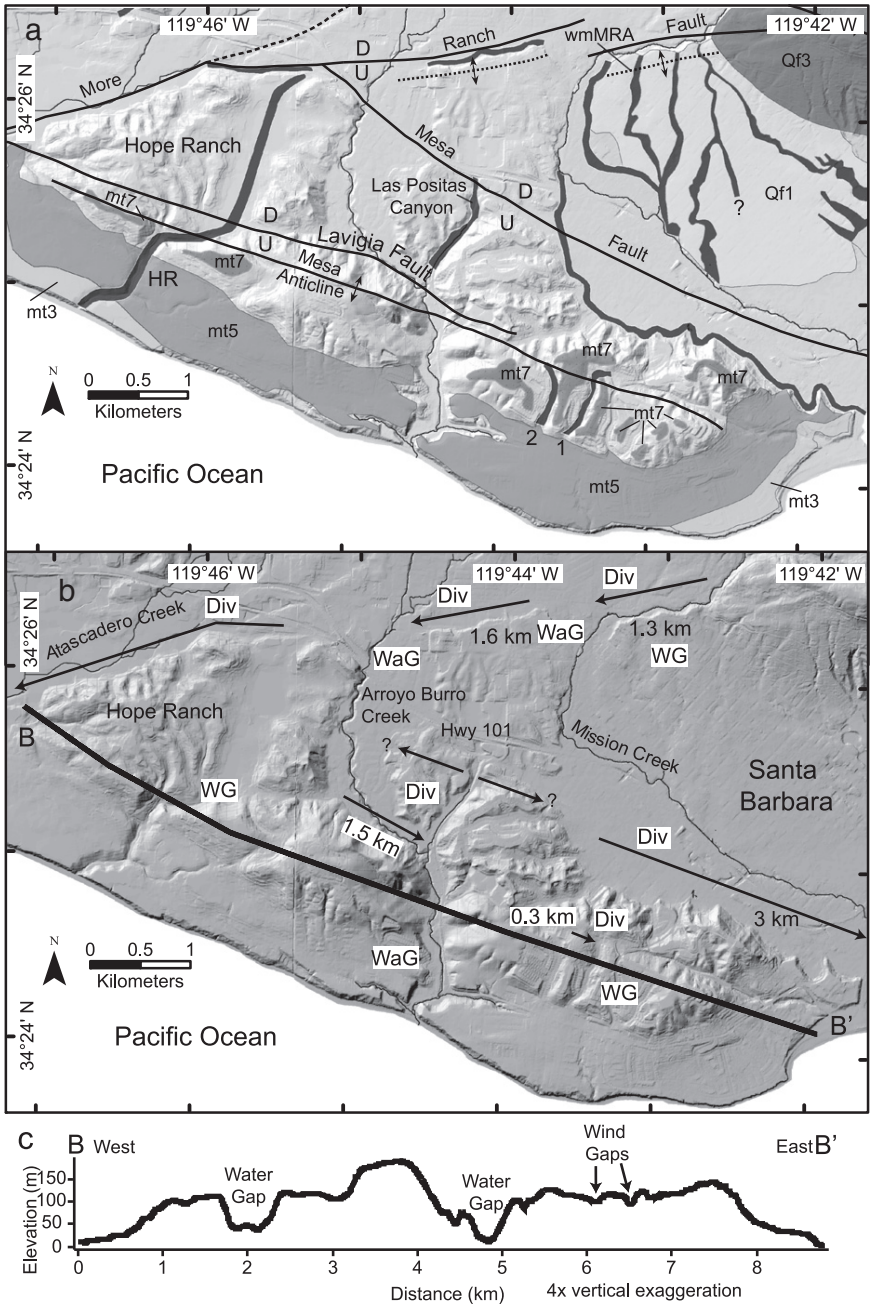

Fig. 6. (a) Geomorphic map of Mesa anticline. Structures and marine terraces are modified after Gurrola (2006). Paleochannels, shown in black, are mapped as part of this investigation. Anticlines include: the Mesa anticline, western most Mission Ridge anticline (wmMRA). Faults include: the More Ranch fault, the Mesa fault, and the Lavigia fault. (b) Map demonstrating paleochannel divergence locations, directions, and approximate magnitudes, marked by arrow location, direction, and length, respectively. Important geomorphic features include: wind gaps (WG), water gaps (WaG), and diversion locations (Div). Cross-section line (B–B′) marks where the topographic profile, shown in (c), is drawn. (c) Topographic profile between B and B′, wind and water gaps are marked.

structure forms. As active faults are rotated, they inherit an unfavorable orientation to accommodate primary stresses, although they are not rendered seismically inactive (Sibson, 1990). The calculated geomorphic indices suggest that east–west oriented structures are the most recent manifestation of tectonic activity in the SBFB (Fig. 13a). However, this does not preclude active movement or fold growth of southeast-northwest oriented structures. Principal stresses are currently accommodated on both sets of southeast-northwest and east–west structures; as rotation continues stress will transfer to mainly the east–west structures.

4.1. Incision rates

Stream incision rates were calculated to test the hypothesis that the SBFB landscape is in a steady state. In a steady state landscape stream incision is in balance with uplift (Adams, 1980). In the SBFB, stream incision rates approximate marine terrace uplift rates (0.4–1.9 m/ka) (Keller and Gurrola, 2000; Gurrola et al., in review). However, the locations of minimal stream incision coincide with some of the higher uplift rates in the field area. For example, the incision rate at Arroyo Burro creek is 0.4 ± 0.1 m/ka and the closest calculated uplift rate, at Santa

Please cite this article as: Melosh, B.L., Keller, E.A., Effects of active folding and reverse faulting on stream channel evolution, Santa Barbara Fold Belt, California, Geomorphology (2013), http://dx.doi.org/10.1016/j.geomorph.2012.12.027

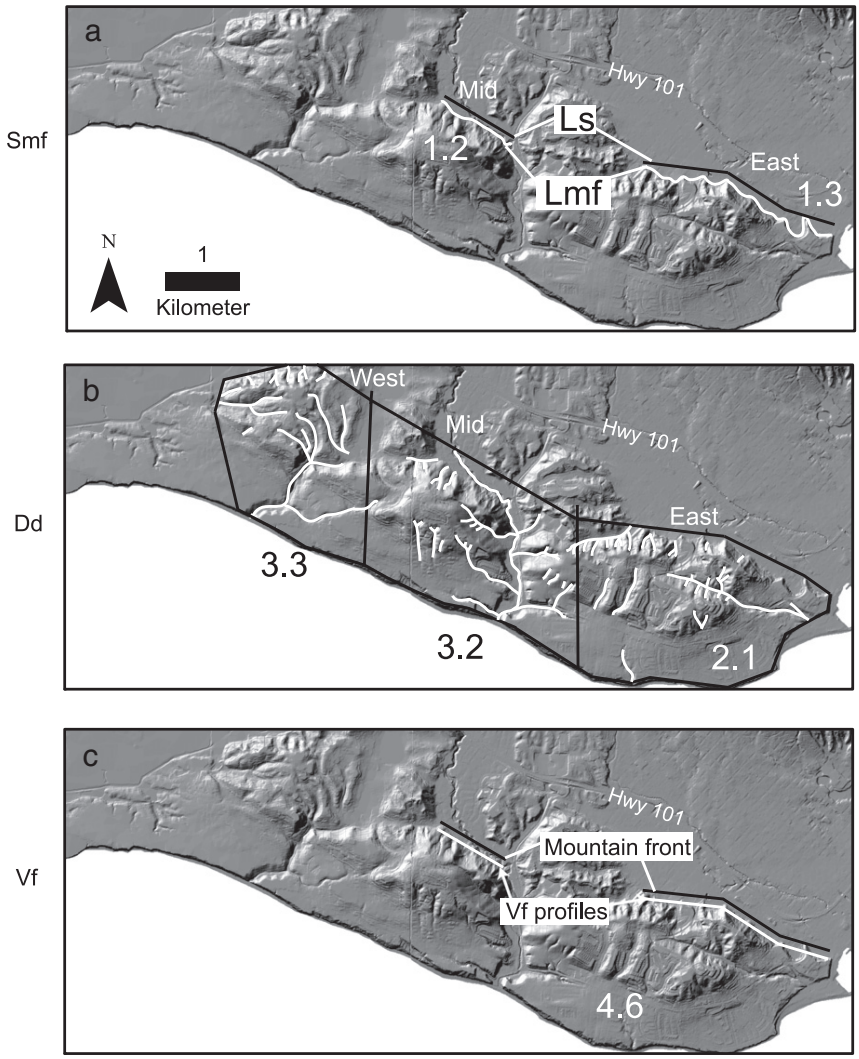

Fig. 7. (a) Map demonstrating how values of mountain front sinuosity were calculated at the Mesa anticline. White lines are sinuous mountain front lengths (Lmf) and black lines are straight-line mountain front lengths (Ls). The fold is divided into middle and east sections due to lack of good measurement locations in the west. Values of Smf are shown. (b) Map demonstrating how values of drainage density were calculated. Boxes represent drainage area in eastern, middle and western segments, white lines represent drainages. Values of Dd are included for each segment. (c) Map demonstrating how valley width to height ratios are calculated. Black lines mark mountain fronts and white lines are locations where valley width to height is measured 0.1 km from the mountain front. The value of Vf is included.

Barbara point, is 1.2–1.3 m/ka (Keller and Gurrola, 2000). Two possible explanations are examined that address why incision rates may vary from uplift rates: 1) variations in base level, and 2) structural control.

Climate changes, particularly sea-level changes during the last ~200 ka, may overprint channel incision values near the coast. For example, streams adjusting to a base-level rise during the last ~20 ka would have been partially filled by alluvium therefore obscuring the long-term incision rate. A future study, using 2-D seismic surveys to measure depth to bedrock at stream channel mouths, may provide maximum channel incision rates.

In addition to climate, stream incision will vary spatially with respect to active structures. If a channel maintains its course, stream incision will be highest where the uplift rate is greatest because tectonic uplift should be matched with erosion in a steady state system (Adams, 1980). Because the incision rate at Sycamore Creek approximates uplift rates calculated by Keller and Gurrola (2000) we infer that the SBFB landscape is in steady state. Maximum uplift occurs in the hanging walls of the Lavigia, Mesa and Mission Ridge faults. The incision rate measurement locations at Arroyo Burro Creek, Hope Ranch Creek and Sycamore Creek are all located in hanging walls; Rattlesnake Creek is located in the footwall of the Mission Ridge fault. Both Rattlesnake Creek and Sycamore Creek are bedrock channels so incision is not obscured by an unknown amount of alluvial fill. We observe maximum stream incision at Sycamore Creek and a 2-fold decrease in incision rate on the opposite side of the Mission Ridge fault at Rattlesnake Creek. These observations highlight the dependence of stream incision on the positions of active structures.

4.2. Paleochannels

In order to determine which streams occupied a particular paleochannel it is assumed that before folding occurred streams were oriented north–south. This allows matching the headwaters of modern streams with paleochannels along the coastal piedmont. In some locations, such as eastern Mission Ridge or western Hope Ranch to Ellwood anticlinorium, branching geometries of paleochannels make the interpretation more difficult. All diversions reported in this study are assumed to be tectonic in origin; this assumption is based on the spatial proximity of abandoned paleochannels heads to active faults. We recognize that stream diversions can occur for a variety of non-tectonic

Please cite this article as: Melosh, B.L., Keller, E.A., Effects of active folding and reverse faulting on stream channel evolution, Santa Barbara Fold Belt, California, Geomorphology (2013), http://dx.doi.org/10.1016/j.geomorph.2012.12.027

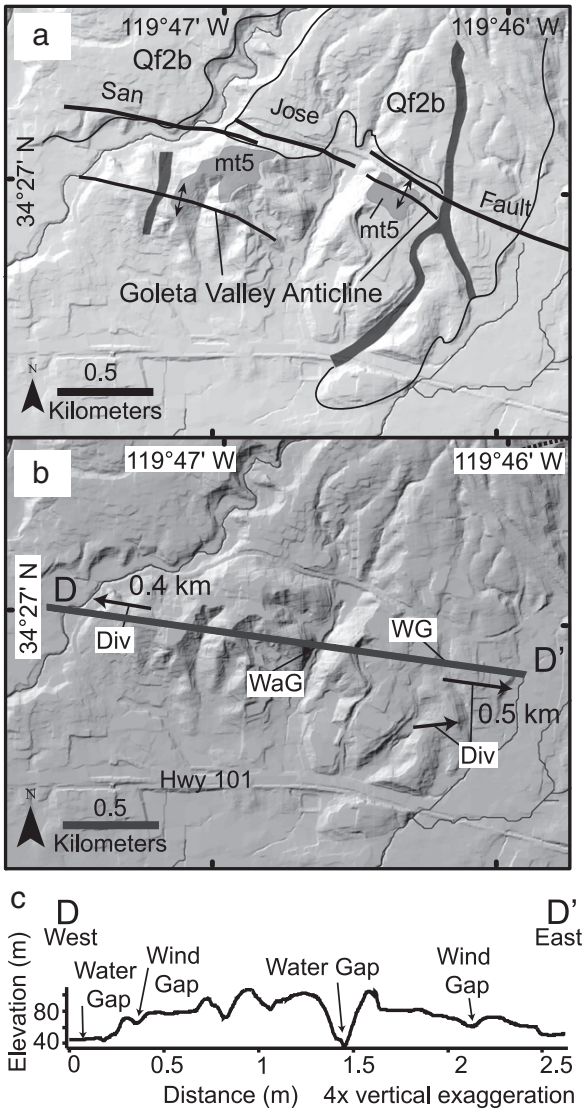

Fig. 8. (a) Geomorphic map of the Goleta Valley anticline. Structures, marine terraces and alluvial fan are modified after Gurrola (2006). Paleochannels, shown in black, are mapped as part of this investigation. Qf2b: 70–100 ka alluvial from Zepeda (1987). (b) Map demonstrating paleochannel diversion locations, directions, and approximate magnitudes, marked by arrow location, direction, and length, respectively. Important geomorphic features include: wind gaps (WG), water gaps (WaG), and divergence locations (Div). Cross-section line (D–D′) marks where the topographic profile, shown in panel (c). (c) Topographic profile between D and D′, wind and water gaps are marked.

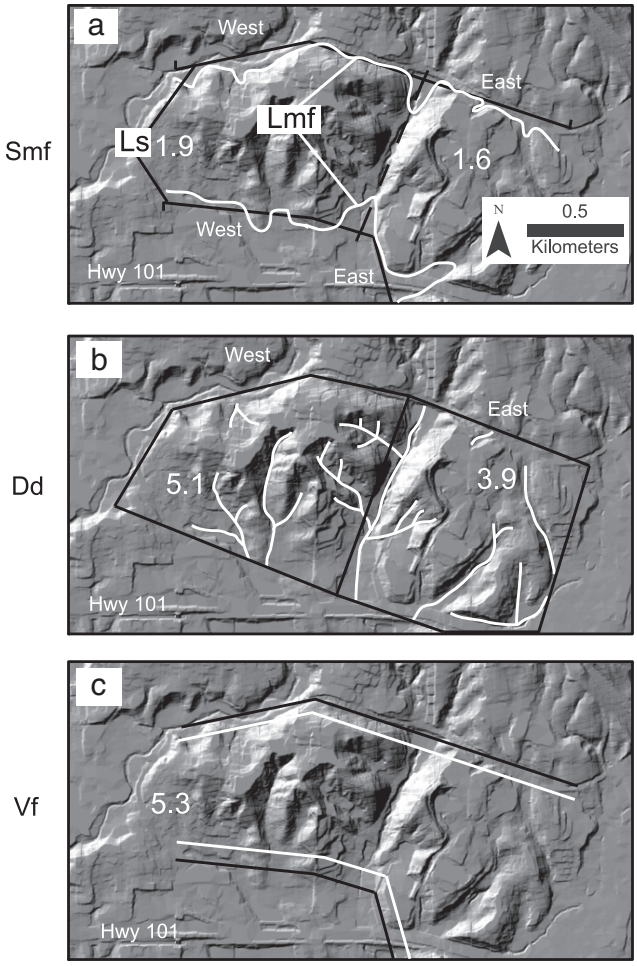

Fig. 9. (a) Map demonstrating how values of mountain front sinuosity were calculated at the Goleta Valley anticline. White lines are sinuous mountain front lengths (Lmf) and black lines are straight-line mountain front lengths (Ls). The anticline is divided into western and eastern sections and values of Smf are included. (b) Map demonstrating how values of drainage density were calculated. Boxes represent drainage area in eastern, middle and western segments, white lines represent drainages. Values of Dd are included. (c) Map demonstrating how valley width to height ratios are calculated. Black line marks mountain front and white line is the location where valley width to height is measured, 0.1 km from the mountain front. Vf value included.

reasons such as channel avulsion or headward incision but do not find sufficient evidence to support either.

4.2.1. Stream diversion index

The stream channel diversion index presented in this paper is based on an approximation of diversion timing and diversion distance along structures. It is shown that although the uncertainties in diversion timing are quite large (e.g. ±75 ka at the Mesa anticline) stream channel diversion indices demonstrate an order of magnitude difference between southeast–northwest and east–west structures (Fig. 13b). Diversion indices are not rates of lateral fold propagation despite the units of m/ka, although diversion distances are a function of fold propagation distances. Keller et al. (1999) suggested that lateral fold propagation might be up to 10 times as fast as vertical fold growth. This idea is supported by the 6.7 km long diversion of Atascadero Creek, the low elevation and poorly dissected morphology of Hope Ranch–Ellwood anticlinorium, and the consistently low values of Smf. The stream diversion index is used as a way to assess relative tectonic activity. Diversion timings alone provide a good first order approach to assess the relative tectonic activity in fold and thrust belts (Fig. 13c). However, the stream diversion index takes an approximation of the minimum magnitude of the fold growth into account, which may be useful during seismic hazard assessments. The validity of this index is supported by the results of Vf, Smf, and Dd (Table 1) and stream diversion timings (Fig. 13c), all of which suggest that east–west structures are more recent than southeast–northwest structures.

4.3. Minimum uplift rates

The uplift rate calculated at western Mission Ridge anticline measures uplift from a depositional surface with a pre-folding elevation that cannot be constrained precisely relative to the geoid. Therefore this is a minimum uplift rate. The value calculated (0.8 ± 0.1 m/ka) is 0.4–0.5 m/ka less than the uplift rate that Keller and Gurrola

Please cite this article as: Melosh, B.L., Keller, E.A., Effects of active folding and reverse faulting on stream channel evolution, Santa Barbara Fold Belt, California, Geomorphology (2013), http://dx.doi.org/10.1016/j.geomorph.2012.12.027

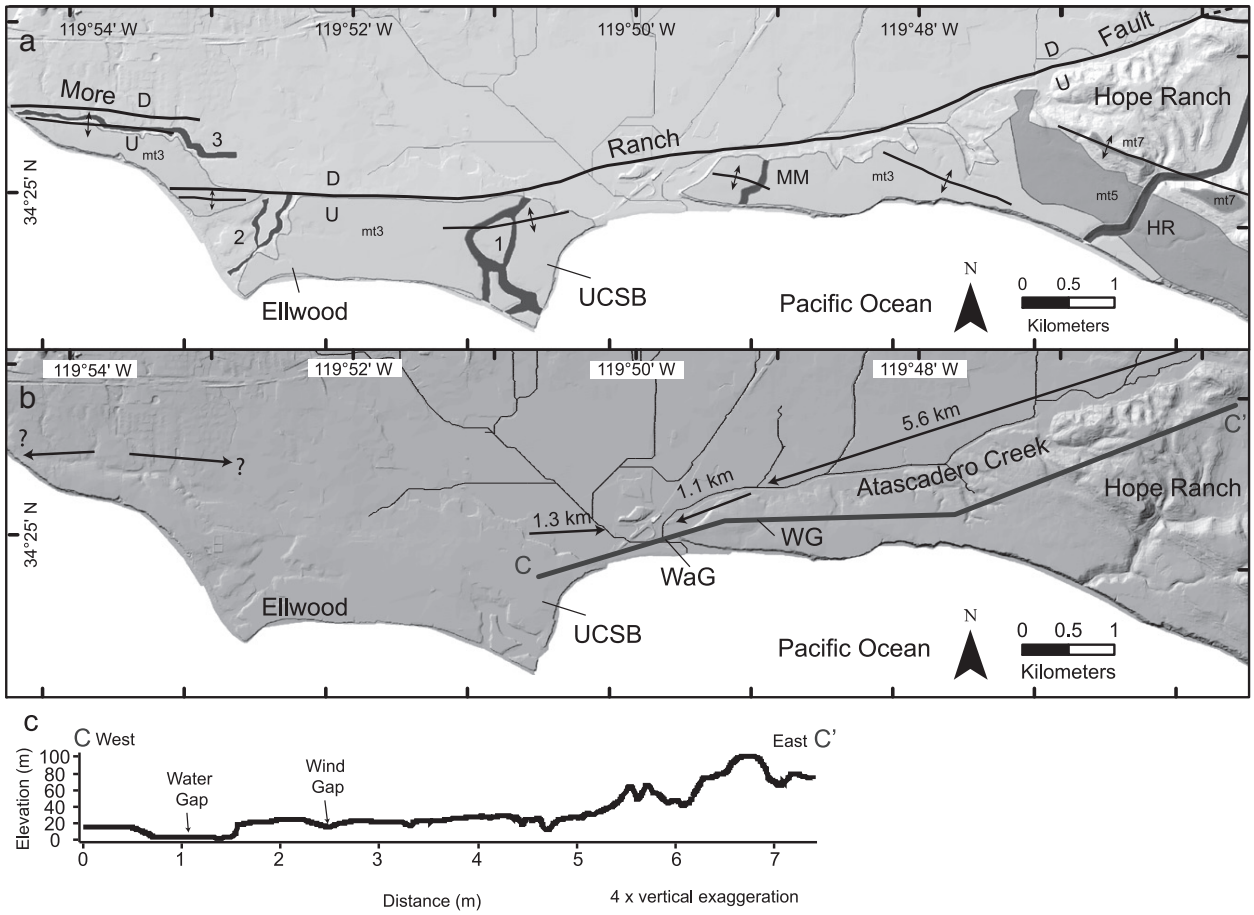

Fig. 10. (a) Geomorphic map of Hope Ranch to Ellwood anticlinorium. Structures and marine terraces are modified after Gurrola (2006). Paleochannels, shown in black, are mapped as part of this investigation. HR: Hope Ranch paleochannel. MM: More Mesa paleochannel. (b) Map demonstrating paleochannel divergence locations, directions, and approximate magnitudes, marked by arrow location, direction, and length, respectively. Important geomorphic features include: wind gaps (WG), water gaps (WaG), and divergence locations (Div). Cross-section line (C–C′) marks where the topographic profile, shown in (c), is drawn. (c) Topographic profile between C and C′, wind and water gaps are marked.

(2000) calculated at the marine terrace platforms on the Mesa anticline (1.2–1.3 m/ka), which is a total surface uplift (sensu England and Molnar, 1990).

The uplift rate calculated for the Mesa fault is a minimum value because the precise age of paleochannel abandonment in not known and paleochannels do not cross the fault. If the paleochannels were to cross the fault they would display a greater vertical offset increasing the uplift rate value. Additionally, it is possible that the uplift rates reported here correspond, in part, to uplift in the footwall block as well as hanging wall block. Finally, uplift on the Mesa fault (0.3–0.4 m/ka) is only partially responsible for the uplift rates of marine terraces to the south (1.2–1.3 m/ka) (Keller and Gurrola, 2000) in the hanging wall of both the Lavigia and Mesa faults.

4.4. Geomorphic analysis of folds

4.4.1. Mission Ridge anticline: southeast–northwest and east–west oriented

The eastward diversion of Montecito Creek and the westward diversion of Mission Creek suggest that Mission Ridge anticline is propagating east and west. This supports the hypothesis that folds propagate to the west but adds the caveat that eastward propagation may still occur. Both of these stream diversions are comparable in distance, 1.8 km at Montecito Creek and 1.3 km at Mission Creek. However, the timing of stream diversion at Montecito Creek may have occurred as early as 139 ka while it is known that Mission Creek was not diverted before 70 ka. This relative timing of diversion supports the hypothesis that the SBFB is most recently dominated by westward propagating east–west oriented structures. Stream diversion index values show a ~2-fold increase from the east to west segments of Mission Ridge anticline, and lend further support to this argument.

Geomorphic indices Smf and Dd calculated along the Mission Ridge anticline show decreased values at the westernmost segment. However, at the eastern and central portions of the structure Smf and Dd values are very similar (Table 1). Vf values were calculated for the entire anticline because of the lack of suitable measurement locations, Mission Ridge anticline has the lowest Vf value found in this study (Fig. 13a, Table 1), lower than Hope Ranch to Ellwood anticlinorium. From the comparison of all geomorphic index values given in Fig. 13 it is suggested that the Mission Ridge anticline is an intermediate age structure. However, due to structural overprinting (i.e. bifurcation of More Ranch fault from Mission Ridge fault) and Smf and Dd values from segments of the structure (Table 1), it is inferred that the eastern and central portions of the structure are relatively old and the westernmost segment is young. The Mission Ridge anticline has experienced segmented and punctuated growth related to timing of offset on the underlying Mission Ridge and More Ranch faults.

4.4.2. Mesa anticline: southeast–northwest oriented

The 3 km eastward diversion of Mission Creek by the eastern segment of the Mesa anticline suggests the fold has propagated toward the east. We did not find any westward diversions of streams related

Please cite this article as: Melosh, B.L., Keller, E.A., Effects of active folding and reverse faulting on stream channel evolution, Santa Barbara Fold Belt, California, Geomorphology (2013), http://dx.doi.org/10.1016/j.geomorph.2012.12.027

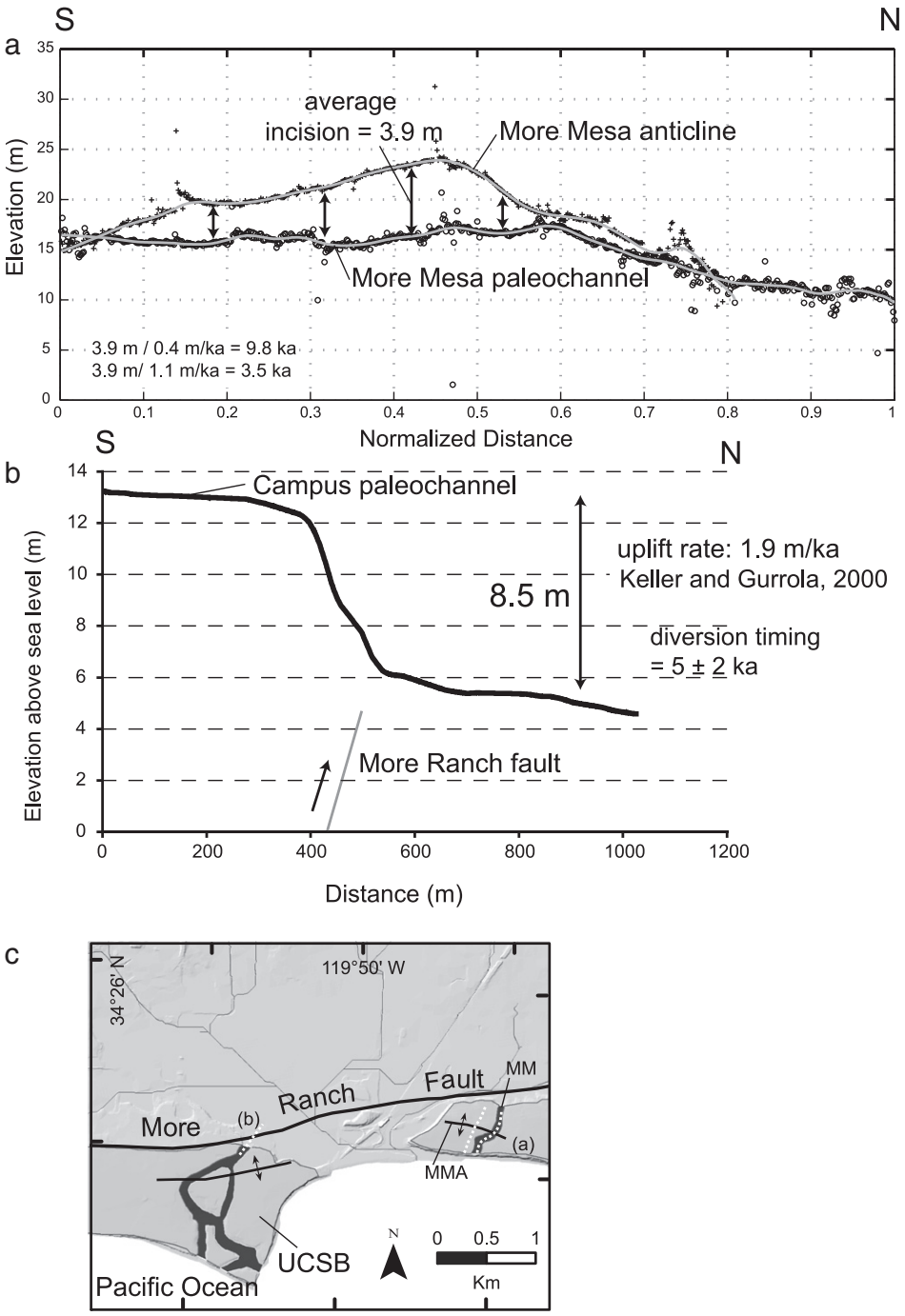

Fig. 11. (a) Raw differential GPS survey taken at More Mesa anticline (part of the Hope Ranch to Ellwood anticlinorium), with 10% r-loess lines (in gray). Arrows indicate amounts of incision (average incision: 3.9 m). (b) Topographic profile of campus paleochannel across the More Ranch fault. Note: five profiles were drawn at this location for average diversion timing of 5 ± 2 ka. (c) Map showing locations where topographic profiles and differential GPS surveys were taken along white lines. MM: More Mesa paleochannel, MMA: More Mesa anticline.

to the Mesa anticline alone, adding additional support to the caveat that streams are diverted east. However, like the Mission Ridge anticline, the westernmost portion of the Mesa anticline overlaps with the Hope Ranch to Ellwood anticlinorium. Therefore, the Atascadero Creek diversion may be related in part to uplift of the Mesa anticline, although uplift of the Hope Ranch to Ellwood anticlinorium is likely the dominant cause. The timing of the 3 km eastward diversion is between 200 and 125 ka, making it the oldest stream diversion in the field area (Fig. 13c). We may be seeing a trend from an early history of eastward diversion in the field area followed by more recent westward diversion. The diversion index is 15–24 m/ka; we are skeptical of this value because it has been overprinted by fluctuations in sea level due to its proximity to the ocean.

Vf and Dd values from the Mesa anticline suggest it is an older structure than east–west structures in the SBFB. Vf and Dd values of 4.6 and 2.8 respectively are high when compared to east–west structures (Table 1, Fig. 13a) but values of Smf are not. One reason for this is the presence of landslides on the forelimb and coastal erosion of the

Please cite this article as: Melosh, B.L., Keller, E.A., Effects of active folding and reverse faulting on stream channel evolution, Santa Barbara Fold Belt, California, Geomorphology (2013), http://dx.doi.org/10.1016/j.geomorph.2012.12.027

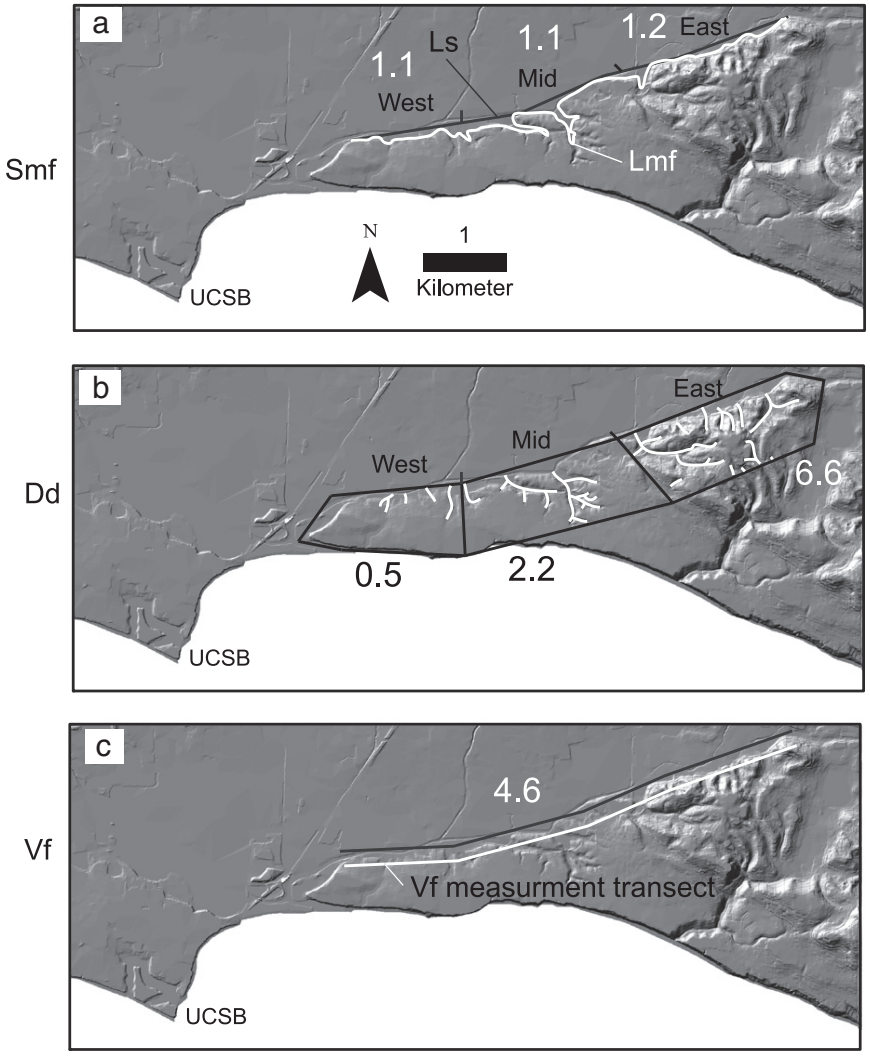

Fig. 12. (a) Map demonstrating how values of mountain front sinuosity were calculated along the Hope Ranch to Ellwood anticlinorium. White lines are sinuous mountain front lengths (Lmf) and black lines are straight-line mountain front lengths (Ls). The fold is divided into western, middle and eastern sections between Hope Ranch and Campus. Values of Smf are included. (b) Map demonstrating how values of drainage density were calculated. Boxes represent drainage area in eastern, middle and western segments, white lines represent drainages. Values of Dd are included. (c) Map demonstrating how valley width to height ratios are calculated. Black line marks mountain front and white line is the location where valley width to height is measured, 0.1 km from the mountain front. The value of Vf is included.

backlimb of the anticline. This reduces the amount of viable locations where measurements can be taken; an Smf value could not be calculated on the western forelimb or any part of the backlimb. For these reasons Smf values at the Mesa anticline do not have tectonic implications. Additionally, increased erosion on the backlimb of the Mesa anticline due to marine platform abrasion decreases the Dd value (Table 1). This explains why values of drainage density decrease to the east where more marine abrasion has occurred; this eastward decrease does not reflect eastward fold propagation.

4.4.3. Goleta Valley anticline: southeast–northwest oriented

Both westward and eastward stream diversions occur at the Goleta Valley anticline, these diversions are of similar magnitudes at 0.5 and 0.4 km, respectively. These diversions occurred no more than 100 ka, making them intermediate age of all the diversions found in the field area (Fig. 13c). The fold morphology is highly dissected, containing two well-developed wind gaps and a water gap. This suggests that the structure is relatively old. The geomorphic index values support this observation.

Geomorphic index values are all significantly higher than other structures and stream diversion index values are the lowest (Table 1, Fig. 13a). Values of Smf and Dd both decrease toward the west, suggesting that the structure has propagated west. Unfortunately, due to the lack of viable locations the anticline could only be divided into two sections. These data are interpreted as supporting the hypothesis that the Goleta Valley anticline is one of the oldest structures in the field area.

4.4.4. Hope Ranch to Ellwood anticlinorium: east–west oriented

All methods used in this study suggest the Hope Ranch to Ellwood anticlinorium is the youngest, most active structure. Three wind gaps and a water gap occur along this structure, the fold shows low relief and low dissection in its elevation profile, with exception of the eastern most segment (Fig. 10c). Paleochannel positions and stream diversions indicate that this structure is rapidly propagating west. Stream diversion occurred between 47 ka and 6 ka (Fig. 13c). The total diversion length is 6.7 km and the stream diversion index is an order of magnitude higher than other values at 183 m/ka (Fig. 13b). Geomorphic index values calculated along the anticlinorium suggest it is propagating west.

The values of Smf and Dd are the lowest in the field area, and Vf is only slightly higher than Mission Ridge anticline (Fig. 13a). Values of

Please cite this article as: Melosh, B.L., Keller, E.A., Effects of active folding and reverse faulting on stream channel evolution, Santa Barbara Fold Belt, California, Geomorphology (2013), http://dx.doi.org/10.1016/j.geomorph.2012.12.027

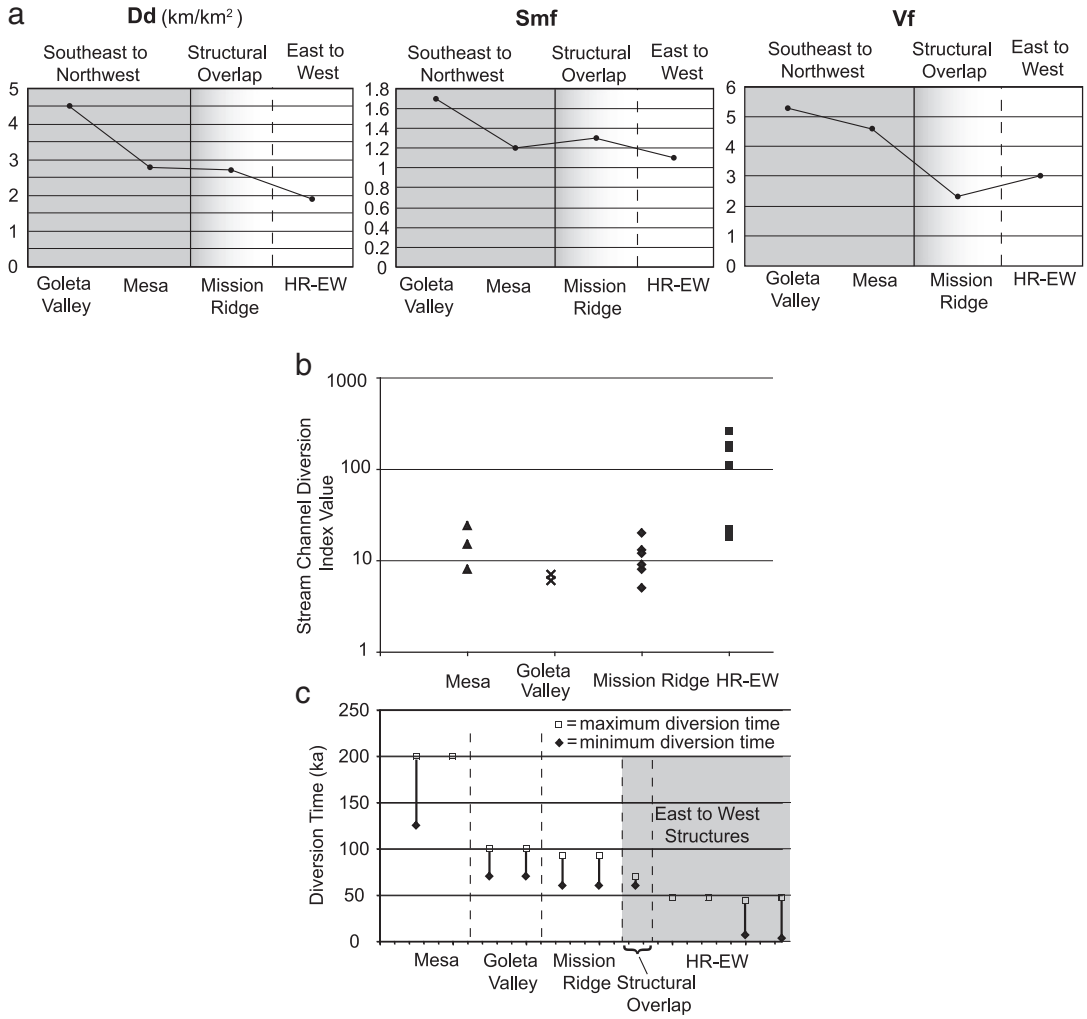

Fig. 13. (a) Graphs showing values of Dd, Smf and Vf for the southeast-northwest and east–west structures. All geomorphic index values decrease on east–west oriented structures suggesting they are the youngest manifestation of deformation in the SBFB. (b) Stream diversion index values for different anticlines in the field area. Greater stream diversion index values correspond to areas undergoing more recent tectonic activity. (c) Ranges in diversion times for different anticlines in the field area. East-to-west oriented structures demonstrate the most recent stream diversions. Structural overlap refers to the area where the More Ranch fault and the Mission Ridge fault join. HR-EW is short for Hope Ranch to Ellwood anticlinorium.

Smf and Dd decrease from east to west (Table 1), supporting the hypotheses that this structure propagates to the west and that deformation in the SBFB dominantly occurs on east–west oriented structures.

5. Conclusions

The dynamic landscape of Santa Barbara is characterized by a series of east–west and southeast–northwest oriented folds that are the surface expression of active blind reverse faults. These two sets of active structures overprint each other at approximately 30º, where east–west structures truncate southeast–northwest structures. Previously determined uplift rates, ages of marine terraces and alluvial fans allow testing of the hypotheses that: the SBFB is in steady state, folds generally propagate west, and that east–west oriented structures are the most recent manifestation of deformation in the SBFB.

Paleochannels were mapped, stream incision calcualted, values of Vf, Smf and Dd measured, and a new stream diversion index presented to test these hypotheses. Stream incision ranges from 0.4 ± 0.1 m/ka to 1.2 ± 0.04 m/ka and previously calculated uplift rates range from 0.4 to 1.9 m/ka (Keller and Gurrola, 2000; Gurrola et al., in review). It is concluded that stream incision keeps pace with uplift in a steady state condition. Complications that arise during the test of steady state are addressed, suggesting that structural position and climate changes strongly influence stream incision values. Stream diversion in the SBFB occurs due to lateral fold propagation, diversion distances range from 0.4 km to 6.7 km; the largest and most recent diversion occurs along an east–west oriented structure in a westward direction. It is inferred that folds dominantly propagate west but that eastward propagation still occurs and suggested that there may be a time dependency to fold propagation direction in the SBFB.

East–west oriented structures have mean values of Vf, Smf, and Dd of 2.7, 1.2, and 2.2 km/km^2, while southeast to northwest structures have mean values of 5.0, 1.5, and 3.7 km/km^2, respectively. Paleochannel diversion timings are loosely constrained but are four times younger along east–west versus southeast–northwest structures. Stream diversion index values range from 6 to 260 m/ka, displaying up to an order of magnitude increase from southeast-northwest to east–west structures. All these data support the hypothesis that east–west faults and folds are the most recently active structures in a rotating micro-block.

East–west structures have a favorable orientation in the north–south shortening regime imposed by the big bend of the San Andreas

Please cite this article as: Melosh, B.L., Keller, E.A., Effects of active folding and reverse faulting on stream channel evolution, Santa Barbara Fold Belt, California, Geomorphology (2013), http://dx.doi.org/10.1016/j.geomorph.2012.12.027

Fault 80 km to the north. Faults and folds form with an east–west orientation and are rotated to a southeast–northwest position, as the SBFB continues to rotate clockwise. Although this new orientation is unfavorable to fault initiation earthquakes still occur on both sets of structures.

Acknowledgments

The first author would like to acknowledge the many helpful reviews by Sarah Hall, as well as reviews by Christie Rowe, which helped with the preparation of this manuscript. Additionally I would like to thank Jessica Thompson, Duane DeVecchio, Andrew Rich and Jiana Ten Brinke for helpful discussions and feedback.

References

Adams, J., 1980. Contemporary uplift and erosion of the Southern Alps, New Zealand. Geological Society of America Bulletin 91, 1–114.
Amos, C.B., Burbank, D.W., Read, S.A.L., 2010. Along-strike growth of the Ostler fault, New Zealand: consequences for drainage deflection above active thrusts. Tectonics 29, TC4021.
Azor, A., Keller, E.A., Yeats, R.S., 2002. Geomorphic indicators of active fold growth: South Mountain–Oak Ridge anticline, Ventura basin, southern California. Geological Society of America Bulletin 114, 745–753.
Bishop, P., 1995. Drainage rearrangement by river capture, beheading and diversion. Progress in Physical Geography 19, 449–473.
Boudiaf, A., Ritz, J.F., Philip, H., 1998. Drainage diversion as evidence of propagating active faults: examples of the El Asnam and Thenia faults, Algeria. Terra Nova-Oxford 10, 236–244.
Bull, W.B., 1977. Tectonic geomorphology of the Mojave Desert, US Geological Survey Contract Report 14-08-001-G-394. Office of Earthquakes, Volcanoes, and Engineering, Menlo Park, CA.
Bull, W.B., 1978. Geomorphic tectonic classes of the south front of the San Gabriel Mountains, California. U.S. Geological Survey Contract Report 14-08-001-G-394. Office of Earthquakes, Volcanoes, and Engineering, Menlo Park, CA.
Bull, W.B., 1991. Geomorphic Response to Climate Change. Oxford University press, New York.
Bull, W.B., McFadden, L.D., 1977. Tectonic geomorphology north and south of the Garlock fault, California. In: Doehring, D.O. (Ed.), Geomorphology in arid regions, Publications in Geomorphology, State University of New York at Binghamton, pp. 115–138.
Burbank, D.W., Anderson, R.S., 2012. Tectonic Geomorphology, 2nd edition. Wiley-Blackwell Science, Oxford.
Burbank, D.W., Meigs, A., Brozovic, N., 1996. Interactions of growing folds and coeval depositional systems. Basin Research 8, 199–223.
Burbank, D.W., McLean, J.K., Bullen, M.E., Abdrakmatov, K.Y., Miller, M.G., 1999. Partitioning of intermontane basins by thrust related folding, Tien Shan, Kyrgyzstan. Basin Research 11, 75–92.
Crowell, J.C., 1979. The San Andreas fault system through time. Journal of the Geological Society 136, 293–302.
DeVecchio, D.E., Keller, E.A., 2008. Earthquake hazard of the Camarillo fold belt: an analysis of the unstudied fold belt in the Southern California "Hot Zone". Final Technical Report, US Geological Survey National Earthquake Hazard Reduction Program (NEHRP), Award Number 07HQGR0040. (52 pp.).
DeVecchio, D.E., Keller, E.A., Fuchs, M., Owen, L.A., 2012. Late Pleistocene structural evolution of the Camarillo fold belt; implications for lateral fault growth and seismic hazard in Southern California. Lithosphere 4, 91–109.
Dibblee, T.W., Jr., 1966. Geology of the central Santa Ynez Mountains, Santa Barbara County, California. California Division of Mines and Geology Bulletin 186, 99, scales 1:62,500 and 1:31,680.
Dibblee, T.W., Jr., 1986. Geologic map of the Santa Barbara quadrangle, Santa Barbara County, California: Dibblee Geological Foundation Map DF-06, (Ehrenspeck, H. E., Ed.), scale 1:24,000.
Dibblee, T.W., Jr., 1987. Geologic map of the Goleta quadrangle, Santa Barbara County, California: Dibblee Geological Foundation Map DF-07,(Ehrenspeck, H.E., Ed.), scale 1:24,000.
England, P.C., Molnar, P., 1990. Surface uplift, uplift of rocks, and exhumation of rocks. Geology 18, 1173–1177.
Gibbs, D.R., 1990. Precipitation Data Report. County of Santa Barbara Flood Control and Water Conservation District, Santa Barbara.
Gilbert, G.K., 1877. Report on the Geology of the Henry Mountains. U.S. Government Printing Office, Washington D.C.
Gupta, S., 1997. Himalayan drainage patterns and the origin of fluvial megafans in the Ganges foreland basin. Geology 25, 11–14.
Gurrola, L. D., 2006. Active tectonics and earthquake hazards of the Santa Barbara Fold Belt, California. PhD Thesis, University of California Santa Barbara.
Gurrola, L.D., Keller, E.A., Chen, J., Owen, L.A., Spencer, J.Q., in review. Tectonic geomorphology of an active fold belt, Santa Barbara, California.
Hornafius, S.J., Luyendyk, B.P., Terres, R.R., Kamerling, M.J., 1986. Timing and extent of Neogene tectonic rotation in the western Transverse Ranges, California. Geological Society of America Bulletin 97, 1476–1487.
Howard, A.D., Kerby, G., 1983. Channel changes in badlands. Geological Society of America Bulletin 94, 739–752.
Humphrey, N.F., Konrad, S.K., 2000. River incision or diversion in response to bedrock uplift. Geology 28, 43–46.
Jackson, J., Norris, R., Youngson, J., 1996. The structural evolution of active fault and fold systems in central Otago, New Zealand: evidence revealed by drainage patterns. Journal of Structural Geology 18, 217–234.
Keller, E.A., Gurrola, L.D., 2000. Earthquake hazard of the Santa Barbara fold belt, California. Final Report to U.S. geological Survey (NEHRP, 99HQGR0081). (Available at www.scec.org/research/98research/98gurrolakeller.pdf).
Keller, E.A., Pinter, N., 2002. Active Tectonics: Earthquakes, Uplift, and Landscape, Prentice Hall Earth Science Series. 2nd edition. Prentice Hall Inc., Upper Saddle River, New Jersey.
Keller, E.A., Zepeda, R.L., Rockwell, T.K., Ku, T.L., Dinklage, W.S., 1998. Active tectonics at Wheeler Ridge, southern San Joaquin Valley, California. Geological Society of America Bulletin 110, 298–310.
Keller, E.A., Gurrola, L.D., Tierney, T.E., 1999. Geomorphic criteria to determine direction of lateral propagation of reverse faulting and folding. Geology 27, 515–518.
Landis, G.P., Gurrola, L.D., Selting, A.J., Mills-Herring, L., 2002. Evaluation of ^{21}N cosmogenic nuclide surface exposure ages from a mid-late Pleistocene alluvial fan and Holocene debris flow, Santa Barbara, CA. Geological Society of America Abstracts with Programs, 34, p. 124.
Luyendyk, B.P., Kamerling, M.J., Terres, R.R., 1980. Geometric model for Neogene crustal rotations in southern California. Geological Society of America Bulletin 91, 211–217.
Meade, B.J., Hager, B.H., 2005. Block models of crustal motion in southern California constrained by GPS measurements. Journal of Geophysical Research 110, B0340.
Medwedeff, D., 1992. Geometry and kinematics of an active, laterally propagating wedge thrust, Wheeler Ridge, California. In: Mitra, S., Fisher, G.W., Phillips, O.M., Stanley, S.M., Strobel, D.F. (Eds.), Structural geology of fold and thrust belts. Johns Hopkins University Press, Baltimore, MD, pp. 3–28.
Minor, S.A., Kellog, K.S., Stanley, R.G., Gurrola, L.D., Keller, E.A., Brandt, T.R., 2009. Geologic map of the Santa Barbara Coastal Plain Area, Santa Barbara County, California: U.S. Geological Survey Scientific Investigations Map 3001, scale 1:25,000.
Muhs, D.R., Simmons, K.R., Schumann, R.R., Groves, L.T., Mitrovica, J.X., Laurel, D., 2012. Sea-level history during the Last Interglacial complex on San Nicolas Island, California: implications for glacial isostatic adjustment processes, paleozoogeography and tectonics. Quaternary Science Reviews 37, 1–25.
Ramsey, L.A., Walker, R.T., Jackson, J., 2008. Fold evolution and drainage development in the Zagros Mountains of Fars Province, SE Iran. Basin Research 20, 23–48.
Seidl, M.A., Dietrich, W.E., 1992. The problem of channel erosion into bedrock. Catena Supplement 23, 101–124.
Sibson, R.H., 1990. Rupture nucleation on unfavorably oriented faults. Bulletin of the Seismological Society of America 80, 1580–1604.
Sieh, K.E., Jahns, R.H., 1984. Holocene activity of the San Andreas fault at Wallace Creek, California. GSA Bulletin 95, 883–896.
Silva, P.G., Goy, J.L., Zazo, C., Bardají, T., 2003. Fault generated mountain fronts in southeast Spain: geomorphologic assessment of tectonic and seismic activity. Geomorphology 50, 203–225.
Sklar, L., Dietrich, W.E., 1998. River longitudinal profiles and bedrock incision models: stream power and the influence of sediment supply. In: Tinkler, K.J., Wohl, E.E. (Eds.), Rivers Over Rock: Fluvial Processes in Bedrock Channels: Am. Geosphys. Union Geophysical Monograph, 107, pp. 237–260.
Walker, R.T., 2006. A remote sensing study of active folding and faulting in southern Kerman province, S.E. Iran. Journal of Structural Geology 28, 654–668.
Wells, D.L., Coppersmith, K.J., 1994. New empirical relationships among magnitude, rupture length, rupture width, rupture area, and surface displacement. Bulletin of the Seismological Society of America 84, 974–1002.
Yeats, R.S., 1986. Active faults related to folding. In: Wallace, R.E. (Ed.), Active Tectonics. National Academy Press, Washington, D.C., pp. 63–79.
Zepeda, R.L., 1987. Tectonic geomorphology of the Goleta–Santa Barbara area, California, M.S. thesis, University of California Santa Barbara.

Please cite this article as: Melosh, B.L., Keller, E.A., Effects of active folding and reverse faulting on stream channel evolution, Santa Barbara Fold Belt, California, Geomorphology (2013), http://dx.doi.org/10.1016/j.geomorph.2012.12.027